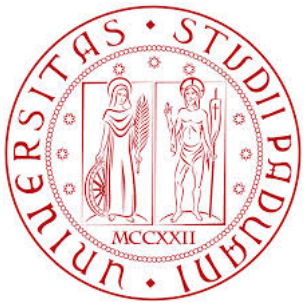


Università degli Studi di Padova

Dipartimento di Fisica e Astronomia
"Galileo Galilei"
Corso di Laurea Magistrale in Fisica

# Development of a smart BSE approach for the calculation of optical properties of complex systems

**Laureando:**
Mario Galante

**Relatore:**
Prof. Paolo Umari

Anno accademico 2014/2015

# Contents

# Introduction

An accurate microscopic description of material properties is essential for the progress of material sciences and condensed matter physics. One of the most common procedures is based on first principles or "ab initio" methods; the main feature of such approach is that is based directly on Schrödinger's or Dirac's equations without the introduction of any phenomenological constant.
Density functional theory (DFT) in many cases provides valid solutions for electronic structure problems treating the electrons as independent particles subdued to an effective single-particle potential ([2], [3]). Although many body perturbation theory (MBPT) produces a significant improvement of DFT results, one-electron mean-field approaches fail to lead to precise evaluations of effects concerning electronic excitations ([4]). The introduction of a wave function dependence to the effective potential (i.e. of a quasi-particle picture), solves the issue in many situations; the consideration of properties such as optical ones requires however two-particle states to be dealt with. The electron-hole interaction is indeed strong enough to allow the formation of bound states known as excitons, consideration of which was proven to be fundamental for the correct prediction of optical absorption spectra. The formulation of an equation of motion for the two-particle Green's function, known as Bethe-Salpeter equation (BSE), allows the inclusion of a two particle interaction and the estimation of excitons quasi-particle energies. Nevertheless, its solution requires the computation of products between matrices with enormous dimensions which thus implies an extremely elevated computational cost, especially in the case of large systems.
In the present work single-particle energies are firstly computed using a DFT calculation within the linear density approximation (LDA). They are then corrected through the solution of a set of equations (Hedin's) which are derived in the Green's functions theory and MBPT framework and simplified through the so called GW approximation. The Bethe-Salpeter equation is then solved in an efficient way through the construction of optimal bases for the calculation of the two particle interaction correction. The selection of the optimal bases elements is realized via the use of different user defined thresholds. Results and efficiency tests for different values of such parameters will be studied.
The information obtained are then exploited in order to efficiently evaluate the imaginary part of the dielectric function using Haydoch recursive method. The dielectric function is directly connected to the adsorption spectrum, which is commonly used to characterize materials.

All the computations are performed with codes contained or developed within the Quantum Espresso suite for electronic structure calculations [19]. The procedure is applied to a system composed by 8 silicon atoms in a cluster structure. We consider different values of the optimal bases thresholds, the number of Haydoch iterations and other parameters and confront our results with others (both experimental and theoretical [17]).

In the first chapter an overview of density functional and single particle Green's function theory within the GW approximation is presented, describing the approach adopted for the evaluation of the single particle energies. The following chapter is focused on the study of optical properties: the Bethe-Salpeter is derived upon the definition of the two particle Green's function theory, along with an expression for the dielectric functions in term of excitation energies. The third chapter is devoted to the several techniques used for the implementation of our method. Finally, several tests on the performance of the approach are presented.

# Chapter 1

# Density functional and Green's functions theories

In this chapter the main theoretical background necessary to the study of a many-electron system will be presented. We will start from the general many-body Hamiltonian of a many-atom system and overview the main problems which must be dealt with. From the simplest independent-particle approximations we will move to density functional theory (DFT) with a particular care to the main approximations adopted. Such approaches are found to be exhaustive in many cases but too inaccurate in others for which more advanced methods are in order [4]. For such purpose we are going to examine Green's functions theory and show how it can be used to considerably improve DFT results. The so-called Hedin's equations are attained and discussed its solution within the GW approximation both self-consistently and not-self-consistently ($G_0W_0$ approximation).

## 1.1 Many-body problems

A many-atom system can be thought as a set of $N$ nuclei and $n$ electrons; we will use the notation $\mathbf{R}_I$ and $\mathbf{r}_i$ with $I = 1, \dots, N$ and $i = 1, \dots, n$ for position operators of the $I$-th ($i$-th) nucleus (electron). The resulting Hamiltonian is, in the units for which $\hbar = m_e = \frac{4\pi}{\varepsilon_0} = e^2 = 1$, of the form

$$\begin{aligned}\hat{H} &= -\sum_{I=1}^{N} \frac{\nabla_{R_I}^2}{2M_I} + \frac{1}{2}\sum_{I,J=1}^{N} \frac{Z_I Z_J}{|\mathbf{R_I} - \mathbf{R_J}|} - \sum_{i=1}^{n} \frac{\nabla_i^2}{2} + \frac{1}{2}\sum_{i,j=1}^{n} \frac{1}{|\mathbf{r_I} - \mathbf{r_j}|} + \sum_{I=1}^{N}\sum_{i=1}^{n} \frac{Z_I}{|\mathbf{R_I} - \mathbf{r_i}|} \\ &= E_{II} + \hat{T} + \hat{V}_{int} + \hat{V}_{ext} \end{aligned} \tag{1.1}$$

where $M_I$ and $eZ_I$ denote the mass and the electric charge of the $I$th nucleus respectively. The term $E_{II}$ is the energy of the subsystem composed by the nuclei alone (first two terms of eq (1.1)), $\hat{T}$ is the electronic kinetic operator, $\hat{V}_{int}$ is the operator relative to electron-electron interactions and $\hat{V}_{ext}$ stands for the electrons-nuclei coupling potential. Since we are dealing with a non-relativistic problem, the equation governing

the dynamics is the Schrödinger equation

$$i\frac{d}{dt}\Psi(\{\mathbf{r}\};t) = \hat{H}\Psi(\{\mathbf{r}\};t) \tag{1.2}$$

where the state is identified by the n-electron wave function $\Psi(\{\mathbf{r}\};t) = \Psi(\mathbf{r_1},\cdots,\mathbf{r_n};t)$. The high number of particles involved makes such equation of really difficult solution, thus some approximations will be necessary. For this purpose it is convenient to define the density $n(\mathbf{r})$ as the mean value of the density operator $\hat{n}(\mathbf{r}) = \sum_{i=1,\cdots,n}\delta(\mathbf{r}-\mathbf{r}')$,

$$n(\mathbf{r}) \equiv \langle\hat{n}(\mathbf{r})\rangle = \frac{\langle\Psi|\,\hat{n}(\mathbf{r})\,|\Psi\rangle}{\langle\Psi|\Psi\rangle} = N\sum_{\sigma}\frac{\int\prod_{j=2}^{n}d^3\mathbf{r_j}\,|\Psi(\mathbf{r},\mathbf{r_2},\cdots,\mathbf{r_n})|^2}{\int\prod_{j=1}^{n}d^3\mathbf{r_j}\,|\Psi(\mathbf{r_1},\cdots,\mathbf{r_n})|^2}. \tag{1.3}$$

Then the total energy of the system can be cast in the form

$$E \equiv \langle\hat{H}\rangle = E_{II} + \langle\hat{T}\rangle + \langle\hat{V}_{int}\rangle + \int d^3\mathbf{r}V_{ext}(\mathbf{r})n(\mathbf{r}). \tag{1.4}$$

Even if the energy $E_{II}$ is essential for the total energy evaluation, it is just a classical additive term in electronic structure theory. In order to correctly estimate the Coulomb interaction energy in extended systems, energy terms must be organized in neutral groups; it is indeed provable that the total energy is finite only if the system is neutral. Therefore, it is customary to define the Hartree energy as the self-interaction energy of the density $n(\mathbf{r})$

$$E_{Hartree} = \frac{1}{2}\int d^3\mathbf{r}d^3\mathbf{r}'\frac{n(\mathbf{r})n(\mathbf{r}')}{|\mathbf{r}-\mathbf{r}'|} \tag{1.5}$$

which allows the derivation of a well-defined expression for the total energy:

$$E = \langle\hat{T}\rangle + (\langle\hat{V}_{int}\rangle - E_{Hartree}) + E_{CC}, \tag{1.6}$$

where the classical Coulomb energy

$$E_{CC} = E_{II} + \int d^3\mathbf{r}V_{ext}(\mathbf{r})n(\mathbf{r}) + E_{Hartree} \tag{1.7}$$

was introduced. In this way all long-range interactions are accounted for in $E_{CC}$, while the middle term contains all short-range ones and is the most challenging to evaluate.

### 1.1.1 Indipendent-electron approximations

One of the most common approaches for the computation of the total energy of an n-electron system is to treat the electrons as particles with no mutual correlations apart from Pauli exclusion principle and to take in account the interaction throughout an effective potential; in other terms, single particle wave functions $\psi_i(\mathbf{x})$ and energies $\epsilon_i^\sigma$

are recovered solving the $n$ coupled eigenproblems

$$\hat{H}_{eff}\psi_i(\mathbf{x}) = \left[-\frac{\nabla^2}{2} + V_{eff}(\mathbf{x})\right]\psi_i(\mathbf{x}) = \varepsilon_i^\sigma \psi_i(\mathbf{x}) \tag{1.8}$$

with $i = 1, \ldots, n$ and $\sigma = \uparrow, \downarrow$. Here $\mathbf{x}$ denotes all coordinates of the particle, in other terms $\mathbf{x} \equiv (\mathbf{r}, \sigma)$. The simplest choice of the effective potential is

$$V_{eff}(\mathbf{x}) = V_{ext}(\mathbf{x}) + \sum_{j=1}^{n} \int d\mathbf{x}' \psi_j^*(\mathbf{x}') \frac{1}{|\mathbf{r} - \mathbf{r}'|} \psi_j(\mathbf{x}') \equiv V_{ext}(\mathbf{x}) + V_{Hartree}(\mathbf{r}); \tag{1.9}$$

the potential $V_{Hartree}(\mathbf{r})$ is usually referred to as the Hartree or direct potential, and such assumption is known as *Hartree approximation*. The direct term embodies the classic Coulomb interaction of one electron with all the others.
The natural evolution of this approach is called *Hartree-Fock approximation* and can be found minimizing the mean value of the Hamiltonian with respect to a generic many-body wave function in the form of a Slater determinant. Then, the ground state of the system is computed via the solution of the $n$ coupled eigenproblems

$$\left[-\frac{\nabla^2}{2} + V_{ext}(\mathbf{r}) + V_{Hartee}(\mathbf{r}) + V_{exc}^i(\mathbf{x})\right]\psi_i(\mathbf{x}) = \epsilon_i^\sigma \psi_i(\mathbf{x}) \tag{1.10}$$

where

$$V_{exc}^i(\mathbf{x}) = \left[\sum_{j=1}^{n} \int d\mathbf{x}' \psi_j^*(\mathbf{x}') \frac{1}{|\mathbf{r} - \mathbf{r}'|} \psi_i(\mathbf{x}')\right] \frac{\psi_j(\mathbf{x})}{\psi_i(\mathbf{x})} \tag{1.11}$$

is called exchange potential. For further details see [7].
The Hartree-Fock approximation is a simple but useful tool, since it constitutes the basics for most of the approaches based on the Kohn-Sham method which is adopted in the present work.

## 1.2 Hohemberg-Kohn theorems and Kohn-Sham Hamiltonian

The scope of this section is to introduce a generalization of the Hartee-Fock approach for the calculation of the ground state of a many-electron system. The fundamental idea we are going to develop is that not only the ground state energy can be computed given the density function, but any property of a many-interacting-particle system can be treated as a functional of the ground state density $n_0(\mathbf{r})$. The formalism constructed upon this concept is known as *density functional theory*. Its foundations are based on two theorems due to Hohenberg and Kohn [2]:

**Theorem 1.** *For any system of interacting particles subdued to an external potential $V_{ext}(\mathbf{r})$, the ground state particle density $n_0(\mathbf{r})$ uniquely determines the potential $V_{ext}(\mathbf{r})$, apart from a constant.*

The Hamiltonian is thus completely determined given the ground state density, as well as all the other properties of the system.

**Theorem 2.** *For any choice of the external potential a universal functional for the energy $E[n(\mathbf{r})]$ can be defined, and the global minimum and its corresponding density of such functional are the exact ground state energy and density.*

The knowledge of such functional is then sufficient to exactly determine all ground state properties of the system. However, no simplification of the original problem has been performed yet and the determination of such functional is everything but straightforward. The most used approach here is to replace the Hamiltonian of the many-body system (1.1) with an easily solvable auxiliary system, like an independent-particle one. Since there is no unique choice of the auxiliary system, nor rigorous proof of its existence for real systems, this method is known as the *Kohn-Sham ansatz* [3]. In particular, the basic assumptions made by Kohn and Sham are the following:

1. (Non-interacting-V-representability) The exact ground state density can be represented by the ground state density of an auxiliary system of non-interacting particles.

2. The auxiliary Hamiltonian has the form

$$\hat{H}^{\sigma} = -\frac{1}{2}\nabla^2 + V_{ext}(\mathbf{x}) + V_{eff}(\mathbf{x}). \tag{1.12}$$

The number density of the auxiliary system can be express in terms of the $N = N^{\uparrow} + N^{\downarrow}$ wave functions $\psi_i(\mathbf{x})$:

$$n(\mathbf{x}) = \sum_{\sigma=\uparrow,\downarrow} \sum_{i=1}^{N^{\sigma}} |\psi_i(\mathbf{x})|^2; \tag{1.13}$$

the independent-particle kinetic energy can thus be written as

$$T_{KS} = -\frac{1}{2} \sum_{\sigma=\uparrow,\downarrow} \sum_{i=1}^{N^{\sigma}} \langle \psi_i(\mathbf{x}) | \nabla^2 | \psi_i(\mathbf{x}) \rangle = \frac{1}{2} \sum_{\sigma=\uparrow,\downarrow} \sum_{i=1}^{N^{\sigma}} |\nabla \psi_i(\mathbf{x})|^2. \tag{1.14}$$

Hence, recovered the expression (1.5) for the Hartree energy, the Kohn-Sham ground state energy functional has the form

$$E_{KS} = T_{KS}[n] + \int d\mathbf{r} V_{ext}(\mathbf{r}) n(\mathbf{r}) + E_{Hartree}[n] + E_{II} + E_{xc}[n]. \tag{1.15}$$

All many-body effects of exchange and correlation are included in the exchange correlation-energy $E_{xc}$, which can be expressed in the notation

$$E_{xc}[n] = \langle \hat{T} \rangle - T_{KS}[n] + \langle \hat{V}_{int} \rangle - E_{Hartree}[n]. \tag{1.16}$$

If the exact form of such potential was known, an exact solution of the Kohn-Sham problem would be possible. In practice some approximate expressions for the potentials

must be adopted.
Now that the Kohn-Sham functional was provided, let us derive the explicit form of the Kohn-Sham Hamiltonian which is usually considered for the actual computation. For such purpose, we consider each term of eq. (1.15) as functional of the density and vary the wave functions in order to find the functional equality

$$\frac{\delta E_{KS}}{\delta \psi_i^*(\mathbf{x})} = \frac{\delta T_{KS}}{\delta \psi_i^*(\mathbf{x})} + \left[\frac{\delta E_{ext}}{\delta n(\mathbf{x})} + \frac{\delta E_{Hartree}}{\delta n(\mathbf{x})} + \frac{\delta E_{xc}}{\delta n(\mathbf{x})}\right] \frac{\delta n(\mathbf{x})}{\delta \psi_i^*(\mathbf{x})}. \tag{1.17}$$

Exploiting the properties of functional derivatives (main features of which will be briefly presented in §1.4.1) it is straightforward to attain the Kohn-Sham equation

$$\left[-\frac{1}{2}\nabla^2 + V_{KS}(\mathbf{x})\right] \psi_i(\mathbf{x}) \equiv \left[-\frac{1}{2}\nabla^2 + V_{ext}(\mathbf{r}) + V_{Hartree}(\mathbf{r}) + V_{xc}(\mathbf{x})\right] \psi_i(\mathbf{x}) = \epsilon_i^\sigma \psi_i(\mathbf{x}) \tag{1.18}$$

where the potentials

$$V_{Hartree}(\mathbf{r}) = \frac{\delta E_{Hartree}}{\delta n(\mathbf{x})} \qquad \text{and} \qquad V_{xc} = \frac{\delta E_{xc}}{\delta n(\mathbf{x})} \tag{1.19}$$

were defined. The single-particle energies $\epsilon_i^\sigma$ and wave functions $\psi_i(\mathbf{x})$ are usually referred to as Kohn-Sham energies and eigenfunctions. It is important to note that the Kohn-Sham eigenvalues are not the real single-particle energies and have in general no physical meaning, exception made for the highest eigenvalue which corresponds to the ionization energy changed of sign (i.e. $-I$) [8]. Nevertheless, Kohn-Sham energies and wave functions can be used to construct well-defined physical quantities, or as the starting point for many-body calculation techniques such as quantum Monte Carlo [9] and many-body perturbation approaches (see §1.4).

## 1.3 Exchange-correlation potentials and pseudopotentials

In order for the Kohn-Sham problem to be solved, explicit expressions for both the exchange-correlation and the external potential must be provided. The reliability of the approach lies completely on the accuracy with which such quantities are estimated. One of the most widely used approximation for the exchange-correlation potential is the *local spin density approximation* (LSDA), in which

$$E_{xc}^{LSDA}[n^\uparrow, n^\downarrow] = \int d^3 n(\mathbf{r}) \epsilon_{xc}^{hom}(n^\uparrow(\mathbf{r}), n^\downarrow(\mathbf{r})). \tag{1.20}$$

In other terms, the exchange-correlation energy is assumed to be in every point equal to the one in a homogeneous electron gas with the same density. Such assumption is legitimized by the fact that in many solids corrections due to the presence of the external potential are not important. In case of unpolarized system, the local density

approximation (LDA) is recovered setting $2n^{\uparrow}(\mathbf{r}) = n(\mathbf{r}) = 2n^{\downarrow}(\mathbf{r})$. Since the exchange part can be analytically evaluated and the correlation energy is accurately calculated with Monte Carlo methods, the functional $E_{xc}$ is universally defined.
The LSDA approach can be actually improved in many different ways. A frequently adopted class of approximations beyond LSDA is composed by *generalized-gradient approximations*: the basic idea is to consider the energy depending on both densities and their gradients, in order to better take account for non-local effects. In particular, it is customary to work with a functional of the generalized form

$$E_{xc}^{GGA}[n^{\uparrow}, n^{\downarrow}] = \int d^3n(\mathbf{r})\epsilon_x^{hom}(n)F_{xc}(n^{\uparrow}, n^{\downarrow}, |\nabla n^{\uparrow}|, |\nabla n^{\downarrow}|, \cdots) \tag{1.21}$$

where $F_{xc}$ is a dimensionless functional that can be analytically evaluated to lowest orders. Such approximations are widely used in chemistry for the fact they allow in many cases the achievement of accurate results on molecular geometries and ground state energies.
In the study of atom clusters, molecules or solids one is usually more interested in the behavior of valence electrons over the core ones, for the fact the latter do not participate to interatomic bounds. Thus, instead of reproducing all-electron (full-) potentials, it is simpler to consider effective potentials, called *pseudopotentials*, which exclude core electrons from the computation taking a mean of their effects on the system. Valence electrons are then to be expressed using pseudo-wavefunctions which can be written with a much smaller number of plane waves (PWs) than the all-electron case. The choice of the pseudopotential depends on the system considered and on the type of computation to be performed. One usually seeks a good compromise between three characteristics:

- Transferability: adaptability to different configurations.
- Softness: the strongest the oscillations of pseudo-wavefunctions are, the highest number of plane waves is required.
- Computational efficiency: it scales with the number of plane waves required.

*Norm-conserving pseudopotentials* (NCPPs) are often generated from "ab initio" calculations on atoms and provide orthonormalized valence pseudofunctions, which imply a good degree of accuracy and a simple application, but sometimes a high computational cost. Such feature can be improved considering a smooth function and an auxiliary function which accounts for the rapid variation of the density around each ion core. These potentials are known as *ultrasoft pseudopontentials* and are often used to enhance computational speed at a cost of a more troublesome implementation.

## 1.4 Single-particle Green's function and Hedin equations

The second quantization formalism is now adopted, in which wave functions are promoted to field operators (see [5] for a complete explanation). Since our objective is the description of a many-electron system we are going to work with fermion-field operators defined as

$$\hat{\Psi}(\mathbf{x}) = \sum_k \psi_k(\mathbf{x}) c_k \qquad \text{and} \qquad \hat{\Psi}^\dagger(\mathbf{x}) = \sum_k \psi_k^*(\mathbf{x}) c_k^\dagger \tag{1.22}$$

and satisfying the anticommutation relations

$$\left\{\hat{\Psi}(\mathbf{x}), \hat{\Psi}^\dagger(\mathbf{x}')\right\} = \delta(\mathbf{x}-\mathbf{x}') \qquad \text{and} \quad \left\{\hat{\Psi}(\mathbf{x}), \hat{\Psi}(\mathbf{x}')\right\} = 0 = \left\{\hat{\Psi}^\dagger(\mathbf{x}), \hat{\Psi}^\dagger(\mathbf{x}')\right\}. \tag{1.23}$$

Here $\mathbf{x}$ and $\mathbf{x}'$ denote both spatial and spin variables, $\psi_k(\mathbf{x})$ is the single-particle wave function, $c_k^\dagger$ ($c_k$) is the fermonic creation (destruction) operator and $k$ runs on all the possible values of the quantum numbers. The Hamiltonian corresponding to the N-electrons system has the form

$$\hat{H} = \int d\mathbf{x} \hat{\Psi}^\dagger(\mathbf{x}) h(\mathbf{r}) \hat{\Psi}(\mathbf{x}) + \frac{1}{2} \int d\mathbf{x} d\mathbf{x}' \hat{\Psi}^\dagger(\mathbf{x}) \hat{\Psi}^\dagger(\mathbf{x}') v(\mathbf{r}, \mathbf{r}') \hat{\Psi}(\mathbf{x}') \hat{\Psi}(\mathbf{x}). \tag{1.24}$$

where

$$h(\mathbf{r}) = -\tfrac{\hbar^2}{2m}\nabla^2 + V(\mathbf{r}) \quad \text{and} \quad v(\mathbf{r}, \mathbf{r}') = \tfrac{e^2}{|\mathbf{r}-\mathbf{r}'|} \tag{1.25}$$

are the one-electron Hamiltonian and the bare Coulomb interaction.
In order to simplify the calculations we study the response of the system under the action of an external scalar potential $U(\mathbf{x}, \mathbf{x}'; t)$ local in time and nonlocal in space; we will also assume it to be Hermitian in the $\mathbf{x}$ variables for any time $t$ and vanishing for $|t| \to \infty$. This is simply a formal tool which allows a compact form of the quantities we are interested in to be reached: once expressed without any dependence from the potential they will be used in the limit of vanishing $U$. From now on the set of spatial and temporal coordinates $(\mathbf{x_1}, t_1)$ will be simply denoted with (1). It is then possibile to introduce the field operator in the interaction picture

$$\hat{\Psi}(1) \equiv \hat{\Psi}_I(\mathbf{x_1}, t_1) = \mathrm{e}^{\frac{i\hat{H}t_1}{\hbar}} \hat{\Psi}(\mathbf{x_1}) \mathrm{e}^{-\frac{i\hat{H}t_1}{\hbar}} \tag{1.26}$$

as well as the interaction Hamiltonian

$$\hat{H}'_I(t) = \mathrm{e}^{\frac{i\hat{H}t}{\hbar}} \hat{H}'(t) \mathrm{e}^{-\frac{i\hat{H}t}{\hbar}} = \int d\mathbf{x} d\mathbf{x}' \hat{\Psi}^\dagger(\mathbf{x}, t^+) U(\mathbf{x}, \mathbf{x}'; t) \hat{\Psi}(\mathbf{x}', t) \tag{1.27}$$

with $t^+ \equiv t + \delta$ ($\delta \to 0^+$) and the formal operator

$$\hat{S} = \exp\left[-\frac{i}{\hbar} \int_{-\infty}^{+\infty} dt \hat{H}'_I(t)\right]. \tag{1.28}$$

The generalized *single-* and *two-particle Green's functions* are defined respectively as

$$G_1(1,2) = -\frac{i}{\hbar}\frac{\langle N|\, T[\hat{S}\hat{\Psi}(1)\hat{\Psi}^\dagger(2)]\,|N\rangle}{\langle N|\, T[\hat{S}]\,|N\rangle} \tag{1.29}$$

and

$$G_2(1,2;1',2') = \left(-\frac{i}{\hbar}\right)^2 \frac{\langle N|\, T[\hat{S}\hat{\Psi}(1)\hat{\Psi}(2)\hat{\Psi}^\dagger(2')\hat{\Psi}^\dagger(1')]\,|N\rangle}{\langle N|\, T[\hat{S}]\,|N\rangle}. \tag{1.30}$$

The state $|N\rangle$ is the ground state of the unperturbed $N$-electron system and $T$ is Wick's time ordering operator. Evidently, the regular definitions displayed in [5] are recovered in the limit of vanishing $U$. We now focus on the single-particle Green's function and overview the derivation of the complete set of equations necessary to describe its behavior. (For further insights see [6]).

### 1.4.1 Dyson's equation

As first step, we define the time evolution operator in the interaction picture as

$$T[\hat{S}(t_a,t_b)] = T\left\{\exp\left[-\frac{i}{\hbar}\int_{t_a}^{t_b} dt\hat{H}_I(t)\right]\right\}. \tag{1.31}$$

The following properties are straightforwardly demonstrated:

- group property
$$T[\hat{S}(t_a,t_c)] = T[\hat{S}(t_a,t_b)]T[\hat{S}(t_b,t_c)]; \tag{1.32}$$

- assuming $t_a > t_1 > t_2 > t_b$, decomposition property
$$T\left[\hat{S}(t_a,t_b)\hat{\Psi}(1)\hat{\Psi}(2)\right] = T[\hat{S}(t_a,t_1)]\hat{\Psi}(1)T[\hat{S}(t_1,t_2)]\hat{\Psi}(2)T[\hat{S}(t_2,t_b)]; \tag{1.33}$$

- and the time derivatives
$$\begin{aligned}\frac{\partial}{\partial t_a}T\left[\hat{S}(t_a,t_b)\right] &= -\frac{i}{\hbar}\hat{H}'_I(t_a)T\left[\hat{S}(t_a,t_b)\right]\\ \frac{\partial}{\partial t_b}T\left[\hat{S}(t_a,t_b)\right] &= \frac{i}{\hbar}T\left[\hat{S}(t_a,t_b)\right]\hat{H}'_I(t_b).\end{aligned} \tag{1.34}$$

Moreover, the time derivative of the field operators yields to the expressions

$$\begin{aligned}\frac{\partial}{\partial t_1}\hat{\Psi}(1) &= -\frac{i}{\hbar}\left[h(1) + \int d3v(1,3)\hat{\Psi}^\dagger(3)\hat{\Psi}(3)\right]\hat{\Psi}(1)\\ \frac{\partial}{\partial t_2}\hat{\Psi}(2)^\dagger &= \frac{i}{\hbar}\left[h(2)\hat{\Psi}^\dagger(2) + \hat{\Psi}^\dagger(2)\int d3v(2,3)\hat{\Psi}^\dagger(3)\hat{\Psi}(3)\right].\end{aligned} \tag{1.35}$$

The notations $v(1,2) = v(\mathbf{r}_1 - \mathbf{r}_2)\delta(t_1,t_2)$, $h(1) = h(\mathbf{r})$, $U(1,2) = U(\mathbf{x}_1,\mathbf{x}_2;t_1)\delta(t_1,t_2)$ were introduced.
We are now going to derive an equation describing the time evolution of the single-particle Green's function. Since its dynamics must not depend on the choice of the ordering of the times $t_1$, $t_2$, one can limit to calculations assuming for instance $t_1 > t_2$. Nevertheless, the role played by the two time variables is different; it is thus necessary to compute the derivatives with respect to both $t_1$ and $t_2$. Only the first will be explicitly calculated here, the second being analogous. The combination of the definition (1.29) and the property (1.33) yields to the formula

$$\begin{aligned} &i\hbar\frac{\partial}{\partial t_1}G_1(1,2) = \\ &= \frac{\partial}{\partial t_1}\left[\theta(t_1-t_2)\frac{\langle N|\, T[\hat{S}(-\infty,t_1)]\hat{\Psi}(1)T[\hat{S}(t_1,t_2)]\hat{\Psi}^\dagger(2)T[\hat{S}(t_2,+\infty)]\,|N\rangle}{\langle N|\, T[\hat{S}]\,|N\rangle}\right]. \end{aligned} \tag{1.36}$$

There are four terms depending on $t_1$: the Heaviside's function $\theta$, the field operator $\hat{\Psi}(1)$ and the evolution operators preceding and following $\hat{\Psi}(1)$. Exploiting the properties $\frac{\partial}{\partial t_1}\theta(t_1-t_2) = \delta(t_1-t_2)$, (1.35) and (1.34) the form

$$\begin{aligned} &\left[i\hbar\frac{\partial}{\partial t_1} - h(1)\right]G_1(1,2) = \delta(1,2) + \\ &\quad + \frac{i}{\hbar}\frac{\langle N|\, T[\hat{S}(-\infty,t_1)]\left[\hat{H}'_I(t_1),\hat{\Psi}(1)\right]T[\hat{S}(t_1,t_2)]\hat{\Psi}^\dagger(2)T[\hat{S}(t_2,+\infty)]\,|N\rangle}{\langle N|\, T[\hat{S}]\,|N\rangle} - \\ &- \frac{i}{\hbar}\int d3v(1,3)\frac{\langle N|\, T[\hat{S}(-\infty,t_1)]\hat{\Psi}^\dagger(3)\hat{\Psi}(3)\hat{\Psi}(1)T[\hat{S}(t_1,t_2)]\hat{\Psi}^\dagger(2)T[\hat{S}(t_2,+\infty)]\,|N\rangle}{\langle N|\, T[\hat{S}]\,|N\rangle} \end{aligned} \tag{1.37}$$

is easily obtained. The commutator on second line can be evaluated using (1.27) and (1.23):

$$\left[\hat{H}'_I(t_1),\hat{\Psi}(1)\right] = \int d34\delta(t_1-t_3)\delta(t_1-t_4)U(4,3)\left[\hat{\Psi}^\dagger(4)\hat{\Psi}(3),\hat{\Psi}(1)\right] \tag{1.38}$$

$$= -i\hbar\int d3U(1,3)\hat{\Psi}(3). \tag{1.39}$$

It is important to keep in mind that the condition $t_1 = t_3$ is implied by the definition of the potentials in the compact notations $U(1,3)$ and $v(1,3)$. This fact, along with the writing $\hat{\Psi}^\dagger(3)\hat{\Psi}(3)\hat{\Psi}(1) \equiv -\hat{\Psi}(1)\hat{\Psi}(3^+)\hat{\Psi}^\dagger(3^{++})$, allows us to obtain the results

$$\begin{aligned} &\left[i\hbar\frac{\partial}{\partial t_1} - h(1)\right]G_1(1,2) - \int d3U(1,3)G_1(3,2) + \\ &\qquad + i\hbar\int d3v(1,3)G_2(1,3^+;2,3^{++}) = \delta(1,2) \end{aligned} \tag{1.40}$$

and

$$\left[-i\hbar\frac{\partial}{\partial t_2}-h(2)\right]G_1(1,2)-\int d3G_1(1,3)U(3,2)+$$
$$+i\hbar\int d3v(2,3)G_2(1,3^{--};2,3^{-})=\delta(1,2); \qquad (1.41)$$

the apex in $3^{\pm}$ indicates that the time variable must be augmented or diminished by a positive infinitesimal. The use of the definition (1.30) was possible thanks to the order in which field operators were organized. At the same time, the analogous result for derivation with respect to $t_2$ was reported. In general both the equations are needed because not all the quantities we consider are granted to be Hermitian. On the other hand, the dynamics is not fully determined because of the presence of the two-particle Green's function $G_2$ which remains unspecified. However, conducting analogous calculations one derives equations of motion for the $G_2$ depending on the three-particle Green's function and this way a whole hierarchy can be constructed.
In order to interrupt the hierarchy and later eliminate any dependence on the potential $U$ *functional derivatives* will be widely used. Let $F[\Psi(x)]$ be a functional with $\delta F[\Psi(x)]$ variation to first order in the small modification $\delta\Psi(x)$ of the argument; then the functional derivative of $F$ is the function of $x$, $\frac{\delta F}{\delta\Psi(y)}$, such that

$$\delta F[\Psi(x)]=F[\Psi(x)+\delta\Psi(x)]-F[\Psi(x)]=\int dy\frac{\delta F}{\delta\Psi(y)}\delta\Psi(y). \qquad (1.42)$$

Most of its properties can be deducted via the analogy with regular derivation in $N$ variables. The ones that will prove to be useful are

- functional derivative property

$$\frac{\delta\Psi(x)}{\delta\Psi(y)}=\delta(x-y); \qquad (1.43)$$

- Leibniz rule:

$$\frac{\delta}{\delta\Psi(y)}\left[F[\Psi(x)]G[\Psi(x)]\right]=\frac{\delta F[\Psi(x)]}{\delta\Psi(y)}G[\Psi(x)]+F[\Psi(x)]\frac{\delta G[\Psi(x)]}{\delta\Psi(y)}; \qquad (1.44)$$

- defined the inverse of $F$ the functional $F^{-1}$ as the functional satisfying the relation

$$\int dzF[\Psi(\xi);x,z]F^{-1}[\Psi(\xi);z,y]=\delta(x-y), \qquad (1.45)$$

  for all $\Psi(\xi)$, the expression

$$\frac{\delta F\left[\Psi(\zeta);x,y\right]}{\delta\Psi(z)}=-\int d\xi d\eta F[\Psi(\zeta);x,\xi]\frac{\delta F^{-1}[\Psi(\zeta);\xi,\eta]}{\delta\Psi(z)}F[\Psi(\zeta);\eta,y]; \qquad (1.46)$$

- chain rule:

$$\frac{\delta F[G[\Psi(x);y]]}{\delta\Psi(x)} = \int dy \frac{\delta F}{\delta G(y)} \frac{\delta G(y)}{\delta\Psi(x)}. \tag{1.47}$$

We now consider $G_1$ as a functional of the external potential $U$, and its first-order variation due to a modification $\delta U$ of the potential is

$$\delta G_1(1,2) = -\frac{i}{\hbar} \frac{\langle N|\, T[\delta\hat{S}\hat{\Psi}(1)\hat{\Psi}^\dagger(2)]\,|N\rangle}{\langle N|\, T[\hat{S}]\,|N\rangle} - G_1(1,2) \frac{\langle N|\, T[\delta\hat{S}]\,|N\rangle}{\langle N|\, T[\hat{S}]\,|N\rangle} \tag{1.48}$$

where

$$\delta\hat{S} = -\frac{i}{\hbar} \int d34 \hat{\Psi}^\dagger(3)\delta U(3,4)\hat{\Psi}(4). \tag{1.49}$$

Hence it is straightforward to obtain the functional derivative identity

$$G_2(1,3;2,3^+) = G_1(1,2)G_1(3,3^+) - \frac{\delta G_1(1,2)}{\delta U(3)} \tag{1.50}$$

for a generic scalar potential $U(3) = \delta(3,4)U(3,4)$, which can be used to truncate the hierarchy of Green's functions and achieve a self-consistent equation of motion for the $G_1$. Explicitly we have

$$\left[ i\hbar\frac{\partial}{\partial t_1} - h(1) - U(1) + i\hbar \int d3 v(1,3) G_1(3,3^+) \right] G_1(1,2) - \\ -i\hbar \int d3 v(1^+,3) \frac{\delta G_1(1,2)}{\delta U(3)} = \delta(1,2) \tag{1.51}$$

and

$$\left[ -i\hbar\frac{\partial}{\partial t_2} - h(2) - U(2) + i\hbar \int d3 v(2,3) G_1(3^-,3) \right] G_1(1,2) - \\ -i\hbar \int d3 v(2^-,3) \frac{\delta G_1(1,2)}{\delta U(3)} = \delta(1,2). \tag{1.52}$$

It is then convenient to rewrite these equations in terms of the *self-energy operator* defined by

$$\Sigma(1,2) = \Sigma_H(1,2) + i\hbar \int d34 v(1^+,3) \frac{\delta G_1(1,4)}{\delta U(3)} G_1^{-1}(4,2) \tag{1.53}$$

$$= \Sigma_H(1,2) + M(1,2) \tag{1.54}$$

and

$$\bar{\Sigma}(1,2) = \Sigma_H(1,2) + i\hbar \int d34 G_1^{-1}(1,4) \frac{\delta G_1(4,2)}{\delta U(3)} v(3,2^-) \tag{1.55}$$

$$= \Sigma_H(1,2) + \bar{M}(1,2). \tag{1.56}$$

Such quantity is a non-local single-particle effective operator which depends on the energy; it takes in account the interaction of one electron with all the others. In particular, one can distinguish between the *Hartree* contribution

$$\Sigma_H(1,2) = \delta(1,2)\left[-i\hbar\int d3v(1,3)G_1(3,3^+)\right] \tag{1.57}$$

and the one of the *mass operators* $M(1,2)$, $\bar{M}(1,2)$. Finally we have the differential form of *Dyson's equation*

$$\left[i\hbar\frac{\partial}{\partial t_1} - h(1) - U(1)\right]G_1(1,2) - \int d3\Sigma(1,3)G_1(3,2) = \delta(1,2) \tag{1.58}$$

or equivalently

$$\left[-i\hbar\frac{\partial}{\partial t_2} - h(2) - U(2)\right]G_1(1,2) - \int d3G_1(1,3)\bar{\Sigma}(3,2) = \delta(1,2). \tag{1.59}$$

Usually only one of the previous two equations is considered, since the other is implied by the condition $\Sigma = \bar{\Sigma}$. Since this form is not particularly helpful form a computational point of view we will use an equivalent integral form in terms of the unperturbed Green's function

$$G_1^{(0)}(1,2) \equiv G_1^{(0)}(\mathbf{r}_1,\mathbf{r}_2;\omega) = \sum_i \frac{\psi_i(\mathbf{r}_1)\psi_i^*(\mathbf{r}_2)}{\omega - \epsilon_i \pm i\eta}. \tag{1.60}$$

Here the index $i$ runs on the possible single-particle eigenstates, each characterized by an energy $\epsilon_i$ and a wave function $\psi_i(\mathbf{r})$, while $\eta$ is a positive infinitesimal inserted for convergency reasons. Such function corresponds to a non-interacting particle, hence satisfies the relation

$$\left[i\hbar\frac{\partial}{\partial t_1} - h(1)\right]G_1^{(0)}(1,2) = \delta(1,2) = \left[-i\hbar\frac{\partial}{\partial t_2} - h(2)\right]G_1^{(0)}(1,2); \tag{1.61}$$

consequently, the inverse function ${G_1^{(0)}}^{-1}$ is given by

$${G_1^{(0)}}^{-1}(1,2) = \left[i\hbar\frac{\partial}{\partial t_1} - h(1)\right]\delta(1,2) = \left[-i\hbar\frac{\partial}{\partial t_2} - h(2)\right]\delta(1,2). \tag{1.62}$$

Thus eqs. (1.58) and (1.59) read

$$\int d3\left[{G_1^{(0)}}^{-1}(1,3) - U(1)\delta(1,3) - \Sigma(1,3)\right]G_1(3,2) = \delta(1,2) \tag{1.63}$$

and

$$\int d3G_1(1,3)\left[{G_1^{(0)}}^{-1}(3,2) - U(2)\delta(3,2) - \bar{\Sigma}(3,2)\right] = \delta(1,2). \tag{1.64}$$

The two expressions contain definitions of the left and right inverse of the Green's function $G_1$: requiring them to coincide implies the relation

$$G_1^{-1}(1,2) = {G_1^{(0)}}^{-1}(1,2) - U(1)\delta(1,2) - \Sigma(1,2) \tag{1.65}$$

and the identification $\Sigma = \bar{\Sigma}$. Henceforth, the integral form of Dyson's equation is attained multiplying eq. (1.65) from the left (right) by $G_1^{(0)}(3,1)$ ($G_1(2,4)$) and integrating over 1 and 2:

$$G_1(1,2) = G_1^{(0)}(1,2) + \int d34 G_1^{(0)}(1,3)\Sigma(3,4)G_1(4,2). \tag{1.66}$$

This equation is now suitable to be solved self-consistently using the unperturbed Green's function $G_1^{(0)}$ as starting point.

### 1.4.2 Vertex, dielectric, polarizability functions and dynamically screened interaction

At this rate, the only term still depending on the external potential $U$ is the self energy. To cancel every remaining reference to the external potential $U$ it is customary to define the following auxiliary quantities:

- the *total potential* is taken to be the sum of the external potential and the bare Coulomb interaction of one electron with all the others; in other terms

$$V(1) = U(1) - i\hbar \int d3 v(1,3) G_1(3,3^+). \tag{1.67}$$

  From such definition it is easily deduced the relation

$$\frac{\delta U(1)}{\delta V(2)} = \delta(1,2) + i\hbar \int d3 v(1,3) \frac{\delta G_1(3,3^+)}{\delta V(2)} \tag{1.68}$$

  which will soon prove to be useful.

- The *scalar "irreducible" vertex function* is defined as

$$\tilde{\Gamma}(1,2;3) = -\frac{\delta G_1^{-1}(1,2)}{\delta V(3)} \tag{1.69}$$

  and using in order equations (1.65), (1.68) and the definitions of the self-energy

terms, it can be cast in the form

$$\tilde{\Gamma}(1,2;3) = -\frac{\delta}{\delta V(3)}\left[{G_1^{(0)}}^{-1}(1,2) - U(1)\delta(1,2) - \Sigma(1,2)\right] =$$
$$= \delta(1,2)\left[\delta(1,3) + i\hbar\frac{\delta}{\delta V(3)}\int d4v(1,4)G_1(4,4^+)\right] + \frac{\delta\Sigma_H(1,2)}{\delta V(3)} + \frac{\delta M(1,2)}{\delta V(3)} =$$
$$= \delta(1,2)\delta(1,3) - \frac{\delta M(1,2)}{\delta V(3)}. \tag{1.70}$$

For the fact the Green's function is proportional to the inverse of an energy, the vertex function can be thought as a quantification of the modification of the energy caused by the presence of the potential. Moreover, exploiting the chain rule (1.47) and the property (1.46) an integral equation for the vertex function can be attained:

$$\tilde{\Gamma}(1,2;3) = \delta(1,3)\delta(2,3) + \int d45\frac{\delta M(1,2)}{\delta G_1(4,5)}\frac{\delta G_1(4,5)}{\delta V(3)} =$$
$$= \delta(1,3)\delta(2,3) - \int d4567\frac{\delta M(1,2)}{\delta G_1(4,5)}G_1(4,6)\frac{\delta G_1^{-1}(1,2)}{\delta V(3)}G_1(7,5) =$$
$$= \delta(1,3)\delta(2,3) + \int d4567\frac{\delta M(1,2)}{\delta G_1(4,5)}G_1(4,6)\tilde{\Gamma}(6,7;3)G_1(7,5). \tag{1.71}$$

We notice that such equation for the irreducible vertex function does not depend on the external potential, whereby the limit $U \to 0$ can be taken. However, it is useful to define its "reducible" form

$$\Gamma(1,2;3) = -\frac{\delta G_1^{-1}(1,2)}{\delta U(3)} \tag{1.72}$$

and it is easy to prove that the corresponding integral equation assumes the form

$$\Gamma(1,2;3) = \delta(1,3)\delta(2,3) + \int d4567\frac{\delta\Sigma(1,2)}{\delta G_1(4,5)}G_1(4,6)\Gamma(6,7;3)G_1(7,5). \tag{1.73}$$

The reducible vertex function can be also formulated in terms of the irreducible one, via equations (1.47), (1.67), (1.46):

$$\Gamma(1,2;3) = \int d4\frac{\delta G_1^{-1}(1,2)}{\delta V(4)}\frac{\delta V(4)}{\delta U(3)} = \tag{1.74}$$
$$= \int d4\tilde{\Gamma}(1,2;4)\left[\delta(4,3) - i\hbar\int d5v(4,5)\frac{\delta G_1(5,5^+)}{\delta U(3)}\right] =$$
$$= \tilde{\Gamma}(1,2;3) + i\hbar\int d4567\tilde{\Gamma}(1,2;4)v(4,5)G_1(5,6)\frac{\delta G_1^{-1}(6,7)}{\delta U(3)}G_1(7,5^+) =$$

$$= \tilde{\Gamma}(1,2;3) - i\hbar \int d4567 \tilde{\Gamma}(1,2;4) v(4,5) G_1(5,6) G_1(7,5^+) \Gamma(6,7;3). \quad (1.75)$$

- The *(longitudinal) dielectric matrix*

$$\epsilon(1,2) = \frac{\delta U(1)}{\delta V(2)} \quad (1.76)$$

along with its inverse function

$$\epsilon^{-1}(1,2) = \frac{\delta V(1)}{\delta U(2)}. \quad (1.77)$$

It embodies the adjustment of the Coumlomb interaction necessary for a variation of the total potential. The inverse dielectric function can also be written in terms of the density operator $\hat{\rho}(1) = \hat{\Psi}^\dagger(1)\hat{\Psi}(1)$ which average corresponds to

$$\langle \hat{\rho}(1) \rangle \equiv \frac{\langle N | \, T[\hat{S}\hat{\rho}(1)] \, | N \rangle}{\langle N | \, T[\hat{S}] \, | N \rangle} = -i\hbar G_1(1,1^+), \quad (1.78)$$

then

$$\epsilon^{-1}(1,2) = \delta(1,2) + \int d3 v(1,3) \frac{\delta \langle \hat{\rho}(3) \rangle}{\delta U(2)} = \delta(1,2) + \int d3 v(1,3) \Pi(3,2). \quad (1.79)$$

Here the *reducible polarizability* $\Pi$ was defined. Moreover, introducing the density deviation operator $\hat{\rho}'(1) = \hat{\rho}(1) - \langle \hat{\rho}(1) \rangle$ and exploiting the definition of the Green's functions (1.29) and (1.30), the following alternative expressions can be found:

$$\begin{aligned} \Pi(1,2) = \frac{\delta \langle \hat{\rho}(1) \rangle}{\delta U(2)} &= i\hbar [G_2(1,2;1^+,2^+) - G_1(1,1^+) G_1(2,2^+)] = \\ &= -i\hbar \frac{\langle N | \, T[\hat{S}\hat{\rho}'(1)\hat{\rho}'(2)] \, | N \rangle}{\langle N | \, T[\hat{S}] \, | N \rangle}. \end{aligned} \quad (1.80)$$

Similarly to the case of the vertex function, it is convenient to single out from the polarizability the component which is irreducible with respect to the bare Coulomb interaction $v$, such is consider $\Pi$ as a functional of the total potential $V$. Thus, the use of the chain rule (1.47) and eq. (1.79) yields to

$$\begin{aligned} \Pi(1,2) = \int d3 \frac{\delta \langle \hat{\rho}(1) \rangle}{\delta V(3)} \frac{\delta V(3)}{\delta U(2)} &= \int d3 \frac{\delta \langle \hat{\rho}(1) \rangle}{\delta V(3)} \left[ \delta(3,2) + \int d4 v(3,4) \frac{\delta \langle \hat{\rho}(4) \rangle}{\delta U(2)} \right] = \\ &= P(1,2) + \int d34 P(1,3) v(3,4) \Pi(4,2) \end{aligned} \quad (1.81)$$

with

$$P(1,2) = \frac{\delta\langle\hat{\rho}(1)\rangle}{\delta V(2)} \tag{1.82}$$

*irreducible polarizability.* $P$ can be directly linked with both the irreducible vertex function and the dielectric matrix; throughout the use of eqs. (1.78), (1.46) and the definition (1.69) it is simply found the result

$$\begin{aligned} P(1,2) &= -i\hbar\frac{\delta G_1(1,1^+)}{\delta V(2)} = i\hbar\int d34 G_1(1,3)\frac{\delta G_1^{-1}(3,4)}{\delta V(2)}G_1(4,1^+) = \\ &= -i\hbar\int d34 G_1(1,3)G_1(4,1)\tilde{\Gamma}(3,4;2), \end{aligned} \tag{1.83}$$

while eqs. (1.76), (1.46) lead to

$$\epsilon(1,2) = \frac{\delta}{\delta V(2)}\left[V(1) - \int d3 v(1,3)\langle\hat{\rho}(3)\rangle\right] = \delta(1,2) - \int d3 v(1,3)\tilde{P}(3,2). \tag{1.84}$$

- Finally the *dynamically screened interaction* is given by

$$W(1,2) = \int d3\epsilon^{-1}(1,3)v(3,2) = v(1,2) + \int d34 v(1,4)\Pi(4,3)v(3,2) \tag{1.85}$$

where eq. (1.77) has been exploited; it represents the interaction between two electrons taking in account for the polarization of the medium. An integral equation for the screened interaction can be attained thanks once again to the chain rule (1.47) and to eq. (1.77):

$$\begin{aligned} W(1,2) &= v(1,2) + \int d345 v(1,4)P(4,5)\epsilon^{-1}(5,3)v(3,2) = \\ &= v(1,2) + \int d34 v(1,3)P(3,4)W(4,2). \end{aligned} \tag{1.86}$$

Furthermore, the definition of the screened interaction allows an expression for the mass operator $M$ (non-Hartree contribution to the self energy) not depending on the external potential $U$ to be found; the use of the chain rule (1.47) and of the properties (1.46), (1.45), along with definitions (1.77) and (1.69) yields indeed to

$$M(1,2) = i\hbar\int d34 v(1^+,3)\frac{\delta G_1(1,4)}{\delta U(3)}G_1^{-1}(4,2) = \tag{1.87}$$

$$= -i\hbar\int d4567 v(1^+,3)\frac{\delta V(5)}{\delta U(3)}G_1(1,6)\frac{\delta G_1^{-1}(6,7)}{\delta V(5)}G_1(7,4)G_1^{-1}(4,2) = \tag{1.88}$$

$$= i\hbar\int d356 v(1^+,3)\epsilon^{-1}(5,3)\tilde{\Gamma}(6,2;5)G_1(6,2) = \tag{1.89}$$

$$= i\hbar\int d34 W(1^+,3)G_1(1,4)\tilde{\Gamma}(4,2;3) \tag{1.90}$$

In conclusion, we have derived expressions for our new quantities which do not depend on the external potential. The limit $U \to 0$ can thus be taken and a closed system of equations in the five variables $G_1$, $P$, $\Gamma$, $M$ and $W$ can be obtained:

$$\begin{cases} \tilde{\Gamma}(1,2;3) = \delta(1,3)\delta(2,3) + \int d4567 \frac{\delta M(1,2)}{\delta G_1(4,5)} G_1(4,6) G_1(7,5) \tilde{\Gamma}(6,7;3) \\ P(1,2) = -i\hbar \int d34 G_1(1,3) G_1(4,1) \Gamma(3,4;2) \\ W(1,2) = v(1,2) + \int d34 v(1,3) P(3,4) W(4,2) \\ M(1,2) = i\hbar \int d34 W(1^+,3) G_1(1,4) \tilde{\Gamma}(4,2;3) \\ G_1(1,2) = G_1^{(0)}(1,2) + \int d34 G_1^{(0)}(1,3) \Sigma(3,4) G_1(4,2). \end{cases} \tag{1.91}$$

These equations are usually called *Hedin equations*, and since no approximation was by far adopted they are exact expressions. Nevertheless, they constitute a problem too difficult to be solved, hence some further assumption is necessary in order to practically use this result.

### 1.4.3 GW approximation

In this work the solution of Hedin's equation is attained within the so called *GW approximation* ([13],[14]). It consists in the generation of expressions for the self-energy as functional of $G_1$ by an iteration process in order to provide a correction to the LDA estimate of the single particle energies. In the previous section we defined the self energy as the sum of an Hartee term and a mass term. However, the former is already accounted for in an LDA approach. Hence, the actual quantity we want to iteratively evaluate is just the mass term: for such reason we are going from now on to refer to the self energy $\Sigma$ as just the mass term $M$.
As a starting point for the method, the condition $\Sigma = 0$ is considered, hence the (first order) vertex function is

$$\tilde{\Gamma}(1,2;3) = \delta(1,3)\delta(2,3). \tag{1.92}$$

This leads to a formula for the irreducible polarizability $P$ in terms of which, together with the bare Coulomb interaction $v$ and $G_1$, the dynamically screened interaction $W$ and the vertex function $\Gamma$ can be expanded. One indeed has

$$W(1,2) = v(1,2) + \int d34 v(1,3) P(3,4) v(4,1) + \dots \tag{1.93}$$

and

$$\tilde{\Gamma}(1,2;3) = \delta(1,3)\delta(2,3) + \delta(1,3) \int d45 G_1(1,4) v(4,5) G_1(5,2) + \dots . \tag{1.94}$$

We are going to truncate the expansion of the vertex function at the first order and then evaluate the reducible polarizability within random phase approximation (RPA). The self-energy $\Sigma$ can also be expanded in terms of $G_1$ and $W$ [13]: our approximation consists in considering only the first order of such expansion, taking then the self-energy to be

$$\Sigma = i\hbar G_1(1,2)W(1^+,2) + (i\hbar)^2 \int d34 G_1(1,3)G_1(4,2)W(1,4)W(3,2) + \dots \quad (1.95)$$

$$\cong i\hbar G_1(1,2)W(1^+,2). \quad (1.96)$$

In summary, we derived the equations

$$\begin{cases} P(1,2) = -i\hbar G_1(1,2)G_1(2,1) \\ \Pi(1,2) = \int d3 P(1,3)(1-vP)^{-1}(3,2) \\ W(1,2) = v(1,2) + \int d34 v(1,3)\Pi(3,4)v(4,2) \\ \Sigma(1,2) = i\hbar W(1,2)G_1(2,1) \\ G_1(1,2) = G_1^{(0)}(1,2) + \int d34 G_1^{(0)}(1,3)\Sigma(3,4)G_1(4,2). \end{cases} \quad (1.97)$$

of which a self-consistent solution is possible, fixing $\Sigma = 0$ for the first step.
In practice, we will deal with an even more simplified system, within the so called "$G_0W_0$" or "one shot $GW$" approximation [15]. Only the first term of the self energy expansion is considered, and the Hedin equations are solved with a not-self-consistent method. In conclusion, the complete scheme for the calculation of the single-particle Green's function is the following:

1. The unperturbed Green's function $G_1^{(0)}$ is evaluated using a DFT calculation within the LDA approximation,

$$G_1^{(0)}(\mathbf{r},\mathbf{r}';\omega) = \sum_i \frac{\psi_i^{\mathrm{LDA}}(\mathbf{r})\psi_i^{\mathrm{LDA}*}(\mathbf{r}')}{\omega - \epsilon_i^{\mathrm{LDA}} \pm i\eta}. \quad (1.98)$$

2. The irreducible polarizability $P$ is computed throughout the formula

$$P(\mathbf{r},\mathbf{r}';\omega) = -\frac{i\hbar}{2\pi}\int d\omega' G_1^{(0)}(\mathbf{r},\mathbf{r}';\omega-\omega')G_1^{(0)}(\mathbf{r},\mathbf{r}';\omega'). \quad (1.99)$$

3. The reducible polarizability $\Pi$ is then estimated as (RPA approximation)

$$\Pi(\mathbf{r},\mathbf{r}';\omega) = \int d\mathbf{r}'' P(\mathbf{r},\mathbf{r}'';\omega)(1-vP)^{-1}(\mathbf{r}'',\mathbf{r}';\omega). \quad (1.100)$$

4. The Coulomb screened interaction is calculated:

$$W(\mathbf{r},\mathbf{r}';\omega) = v(\mathbf{r},\mathbf{r}') + \int d\mathbf{r}'' d\mathbf{r}''' v(\mathbf{r},\mathbf{r}'')\Pi(\mathbf{r}'',\mathbf{r}''';\omega)v(\mathbf{r}''',\mathbf{r}'). \quad (1.101)$$

5. Finally, the self-energy is evaluated:

$$\Sigma_{G_0W_0} = \frac{i}{2\pi} \int d\omega' G_1^{(0)}(\mathbf{r}, \mathbf{r}'; \omega + \omega') W(\mathbf{r}, \mathbf{r}'; \omega') e^{-i\omega'\eta}. \tag{1.102}$$

A correction to single-particle LDA energies can then be applied:

$$E_n \simeq \epsilon_n^{LDA} + \langle \Sigma_{G_0W_0}^n \rangle - \langle V_{xc}^n \rangle : \tag{1.103}$$

the LDA exchange-correlation correction is substituted with the more accurate self energy correction. Such estimate proves to be much more accurate than the LDA one in the computation of gap energies in solids [4].

# Chapter 2

# Optical properties of semiconductors and Bethe-Salpeter equation

The primary way to probe electric and optical properties of materials is spectroscopy: wavelengths for vibrational modes are found to be within the infrared ($1000 \div 3000$ $\text{cm}^{-1}$), while energies relative to electronic or excitonic transitions are of the order of the $eV$. Our study will be focused on the interaction of an external light field with excitations in the system. In particular, we are interested in the evaluation of the macroscopic dielectric tensor $\varepsilon_M$ defined as

$$\mathbf{D}(\mathbf{k};\omega) = \varepsilon_M(\mathbf{k};\omega)\mathbf{E}(\mathbf{k};\omega). \tag{2.1}$$

$\mathbf{D}$ and $\mathbf{E}$ stand for the displacement vector and the total electric field respectively. The energy dispersion in the crystal is directly connected to the imaginary part of such tensor, for the computation of which the knowledge of the excitation energies is necessary.
In this chapter some methods, within linear response theory, to compute both infrared and optical spectrum of a crystal will be presented.

## 2.1 Infrared contributions to the dielectric function

We now analyze the linear response of a crystalline lattice to an external electric field $\mathcal{E}$ using the frozen-phonon method [10]. This approach regards a distorted crystal as a new crystal with a lower symmetry than the undistorted one, thus a DFT calculation is performed to compute the total energy of the different atom configurations and a unified approach for lattice dynamics is provided.
Defined $u_i^\mu$ as the displacement of the $i$-th atom with $i = 1, \ldots, N$ in the direction

$\mu = 1, 2, 3$, the equation of motion of the crystal is given by

$$m_i \ddot{u}_i^\mu = -\left(\frac{\partial^2 E_{tot}}{\partial u_i^\mu \partial u_j^\nu}\right)\Bigg|_{u_i^\mu=0=u_j^\nu} u_j^\nu - \left(\frac{\partial^2 E_{tot}}{\partial u_i^\mu \partial \mathcal{E}_\alpha}\right)\Bigg|_{u_i^\mu=0=\mathcal{E}_\alpha} \mathcal{E}_\alpha = \tag{2.2}$$

$$= -\sqrt{m_i m_j} D_{\mu\nu}^{i,j} u_j^\nu + Z_{i\mu}^{\alpha\,*} \mathcal{E}_\alpha, \tag{2.3}$$

where $m_i$ is the mass of the $i$-th atom and the indexes $i, j$ run on the different atoms $1, \ldots, N$ in a cell while $\mu, \alpha$ on the directions $1, 2, 3$. It is customary to denominate the quantities

$$D_{\mu\nu}^{i,j} = \frac{1}{\sqrt{m_i m_j}} \left(\frac{\partial^2 E_{tot}}{\partial u_i^\mu \partial u_j^\nu}\right)\Bigg|_{u_i^\mu=0=u_j^\nu} \quad \text{and} \quad Z_{i\mu}^{\alpha\,*} = -\left(\frac{\partial^2 E_{tot}}{\partial u_i^\mu \partial \mathcal{E}_\alpha}\right)\Bigg|_{u_i^\mu=0=\mathcal{E}_\alpha} \tag{2.4}$$

*dynamical matrix* and *Born effective charge* respectively. The diagonalization of the dielectric matrix, which has dimension $3N \times 3N$ provides the eigenvalues $-\omega_n^2$ and eigenvectors $e_{i\mu}^n$ of the vibrational modes of the system. It is possible to show that the imaginary part of the dielectric tensor can be computed using the expression

$$\Im(\varepsilon_{\alpha\beta}(\omega)) = \frac{4\pi^2}{\Omega} \sum_{n=1}^{3N} \sum_{i,j=1}^{N} \sum_{\mu,\nu=1}^{3} \frac{1}{2\omega_n} \frac{e_{i\mu}^n}{m_i} \frac{e_{j\nu}^n}{m_j} Z_{i\mu}^{\alpha\,*} Z_{j\nu}^{\beta\,*} \delta(\omega - \omega_n) \tag{2.5}$$

with a cell of volume $\Omega$. As a consequence, the knowledge of the effective charges and of the eigenvectors and eigenvalues of the dynamical matrix allow an estimate of the infrared spectrum to be attained.

## 2.2 BSE and excitonic transitions

This section is dedicated to the study of bound electron-hole states, known as *excitons*. After a brief explanation of their main features, the equation (BSE) from which their energies will be attained is derived and then formulated within the GW approximation.

### 2.2.1 Excitons

The term *exciton* refers to a bound state formed by an electron and a hole. This quasi-particle is created when a photon promotes an electron from the valence band to the conduction one thus creating a vacancy in the valence band, i.e. a hole. For the fact the hole can be seen as a particle with positive electric charge, there is a Coulombian attraction between the electron and the hole. On the other hand, such interaction is screened by the remaining electrons. As a consequence, the presence of the interaction between the two particles implies a lowering of the energy of the two-particle state composed by the electron-hole couple, and thus the formation of a bond state.
It is customary to distinguish between the cases of strongly and weakly bounded excitons. In systems like ionic crystals the electron-hole interaction is strong enough to

localize the two particles in the same or nearest-neighbor unit cells; the weakness of the electronic screening leads to a tight bonding between the electron and the hole, and such excitons are known as *Frenkel excitons*. On the contrary, in most semiconductors the dielectric constant is large because of the Coulomb interaction is severely screened by valence electrons; the electron-hole bound is consequently weak and the exciton is not strictly localized. In the present work we are going to focus on this latter type of quasi-particles, called *Wannier(-Mott) excitons* [11]. In addition, we are going to examine only direct transitions: the momentum of the hole has the same modulus of the one of the electron, but opposite direction. In other terms, there is no momentum transfer during the process.
Since our objective is to consider the effects of excitons on absorption spectra, it is important to note that under such hypothesis not all excitons are relevant. If the spin orbit coupling is not considered, only excitons with a spin-triplet-state can be actually created by the incidence of a photon [12]. Excitons with a spin-singlet-state correspond indeed to forbidden transitions. In order to prove that, let us consider the matrix element corresponding to a transition from the N-electron ground state to a state equal to the ground state apart form having an electron in the conduction band $c$ and a hole in the band $v$. We suppose the system to be homogenous with all electronic levels occupiable by two electrons (one spin-up, one spin-down). The two Slater determinants differ only for the part concerning the excited electron and the other electron with which it shares the band $v$ in the ground state. The relevant spin components of the two states are then

$$\begin{gathered}\Phi_{GS}(\mathbf{r_1},\mathbf{r}_2)=\frac{1}{2}\left[\varphi_{v\uparrow}(\mathbf{r}_1)\varphi_{v\downarrow}(\mathbf{r}_2)-\varphi_{v\downarrow}(\mathbf{r}_1)\varphi_{v\uparrow}(\mathbf{r}_2)\right]\\ \text{and}\\ \Phi_{EXC}(\mathbf{r_1},\mathbf{r}_2)=\frac{1}{2}\left[\varphi_{v\uparrow}(\mathbf{r}_1)\varphi_{c\downarrow}(\mathbf{r}_2)-\varphi_{v\downarrow}(\mathbf{r}_1)\varphi_{c\uparrow}(\mathbf{r}_2)\right].\end{gathered} \tag{2.6}$$

The transition matrix element can then be cast in the form

$$\begin{aligned}\langle GS|\,\hat{\mathbf{r}}\,|EXC\rangle &= \frac{1}{4}\int d^3r_1d^3r_2\left[{\varphi_{v\uparrow}}^*(\mathbf{r}_1){\varphi_{c\downarrow}}^*(\mathbf{r}_2)-{\varphi_{v\downarrow}}^*(\mathbf{r}_1){\varphi_{c\uparrow}}^*(\mathbf{r}_2)\right]\cdot\\ &\cdot\,\hat{\mathbf{r}}\left[\varphi_{v\uparrow}(\mathbf{r}_1)\varphi_{v\downarrow}(\mathbf{r}_2)-\varphi_{v\downarrow}(\mathbf{r}_1)\varphi_{v\uparrow}(\mathbf{r}_2)\right]=\\ &=\int d^3r\left[\varphi^*_{v\downarrow}(\mathbf{r})\varphi_{c\downarrow}(\mathbf{r})-\varphi^*_{v\uparrow}(\mathbf{r})\varphi_{c\uparrow}(\mathbf{r})\right]\mathbf{r}.\end{aligned} \tag{2.7}$$

For the fact the system must be invariant under exchange of spin variables the transition amplitude for the spin-up and spin-down case is equal, then the total matrix element is vanishing.
In summary, our analysis will be valid for Wannier excitons corresponding to direct transitions with final triplet-spin-state.

### 2.2.2 Bethe-Salpeter equation

Let us recall the definition of the two-particle Green's function given in §1.3:

$$G_2(1,2;1',2') = \left(-\frac{i}{\hbar}\right)^2 \frac{\langle N|\, T[\hat{S}\hat{\Psi}(1)\hat{\Psi}(2)\hat{\Psi}^\dagger(2')\hat{\Psi}^\dagger(1')]\,|N\rangle}{\langle N|\, T[\hat{S}]\,|N\rangle}. \tag{2.8}$$

The purpose of this section is to derive an equation of motion for such function analogous to Dyson's equation for the single-particle Green's function and to describe the approach for its solution given by Rohlfing and Louie [17]. More precisely, we are looking for an equation in terms of the two-particle correlation function

$$L(1,\mathbf{x}'t;2,\mathbf{x}t^+) = -G_2(1,\mathbf{x}'t;2,\mathbf{x}t^+) + G_1(1,2)G_1(\mathbf{x}'t,\mathbf{x}t^+) = \frac{\delta G_1(1,2)}{\delta U(\mathbf{x},\mathbf{x}';t)} \tag{2.9}$$

where the identity (1.50) was recalled. In order to recover an integral equation for the correlation function eq. (1.65) must be modified: instead of the scalar potential $U(3)$ a potential of the form $U(3,4) \equiv U(3,4)\delta(t_3 - t_4)$ must be considered. Such expression, along with (1.46), (1.47) yields to

$$\begin{aligned}
L(1,\mathbf{x}'t;2,\mathbf{x}t^+) &= -\int d34 G_1(1,3)\frac{\delta G_1^{-1}(3,4)}{\delta U(\mathbf{x},\mathbf{x}';t)}G_1(4,2) = \\
&= \int d34 G_1(1,3)\left[\delta(t_3-t_4)\delta(t_4-t)\delta(\mathbf{x}_3,\mathbf{x})\delta(\mathbf{x}_4,\mathbf{x}') + \frac{\delta\Sigma(3,4)}{\delta U(\mathbf{x},\mathbf{x}';t)}\right]G_1(4,2) = \\
&= G_1(1,\mathbf{x}t)G_1(\mathbf{x}'t,2) + \int d3456 G_1(1,3)G_1(4,2)\frac{\delta\Sigma(3,4)}{\delta G_1(5,6)}L(5,\mathbf{x}'t;6,\mathbf{x}t^+).
\end{aligned} \tag{2.10}$$

A more compact form can be achieved defining the kernel

$$\Xi(3,6;4,5) = \frac{\delta\Sigma(3,4)}{\delta G_1(5,6)} \tag{2.11}$$

which represents an effective two-particle interaction. Noting that eq. (2.9) can be easily generalized to arbitrary time variables $t$ and $t'$, the *Bethe-Salpeter equation* (BSE) for $L$ is attained

$$L(1,2;1',2') = G_1(1,2')G_1(2,1') + \int d3456 G_1(1,3)G_1(4,1')\Xi(3,5;4,6)L(6,2;5,2). \tag{2.12}$$

This is the fundamental equation to be solved in order to obtain informations on electron-hole excitations, which are transitions that do not alter the total number $N$ of electrons, namely $|N,0\rangle \to |N,S\rangle$. Bound exciton states were proven to give significant contributions to the optical spectrum in many systems and to provide results much more similar to experimental data than the ones of the independent-particle spectrum. Since the absence of the two particle interaction would imply the correlation function

to be just the product of two single-particle Green's functions, the notation

$$L_0(1,2;1',2') \equiv G_1(1,2')G_1(2,1') \tag{2.13}$$

is adopted. We will also work under the so called *quasi-particle approximation*, in the sense that each single-particle Green's function will be assumed of the form

$$G_1(\mathbf{x}_1,\mathbf{x}_2;\omega) \simeq \sum_k \frac{\psi_k(\mathbf{x}_1)\psi_k^*(\mathbf{x}_2)}{\omega - \epsilon_k \pm i\delta}, \tag{2.14}$$

with $\delta \to 0^+$. The two-particle Green's function can be divided into six contributions, depending on the ordering of the time variables. Four of them correspond to the creation-annihilation process of two particles and two holes, while the remaining two of one particle and one hole. In our study we are interested in the last case, more precisely in the case of simultaneous creation and annihilation in which the four time variables can be reduced to just one independent for the absence of external fields. Under these hypotheses it is possible (appendix G of [6]) to apply a Fourier transform and to write the expressions

$$L_0(1,2;1,',2';\omega) = i\sum_{v,c}\left[\frac{\psi_c(\mathbf{x}_1)\psi_v^*(\mathbf{x}_{1'})\psi_v(\mathbf{x}_2)\psi_c^*(\mathbf{x}_{2'})}{\omega-(E_c-E_v)} - \frac{\psi_v(\mathbf{x}_1)\psi_c^*(\mathbf{x}_{1'})\psi_c(\mathbf{x}_2)\psi_v^*(\mathbf{x}_{2'})}{\omega+(E_c-E_v)}\right] \tag{2.15}$$

and

$$L(1,2;1',2';\omega) = i\sum_{S}\left[\frac{\chi_S(\mathbf{x}_1,\mathbf{x}_{1'})\chi_S^*(\mathbf{x}_{2'},\mathbf{x}_2)}{\omega-\Omega_S} - \frac{\chi_S(\mathbf{x}_2,\mathbf{x}_{2'})\chi_S^*(\mathbf{x}_{1'},\mathbf{x}_1)}{\omega+\Omega_S}\right] \tag{2.16}$$

where the infinitesimal terms are omitted for sake of clarity. The sums in (2.15) on $c$ and $v$ run on all conduction and valence states respectively. On the other hand, the formula (2.16) is valid for long-lived transitions $S$, to each of which is associated an energy $\Omega_S$ and an electron-hole amplitude

$$\chi_S(\mathbf{x},\mathbf{x}') = -\langle N,0|\,\hat{\Psi}^\dagger(\mathbf{x}')\hat{\Psi}(\mathbf{x})\,|N,S\rangle\,. \tag{2.17}$$

Considering the expansion (1.22), it is easy to see that $\chi_S$ will be non-zero only if the creation operators are applied to an empty conduction or an occupied valence state. Consequently we can expand the electron-hole amplitude in the form

$$\chi_S(\mathbf{x},\mathbf{x}') = \sum_{v}^{occ}\sum_{c}^{empty}\left[A_{vc}^S\psi_c(\mathbf{x})\psi_v^*(\mathbf{x}') + B_{vc}^S\psi_v(\mathbf{x})\psi_c^*(\mathbf{x}')\right]. \tag{2.18}$$

Each excitation $S$ is identified by the coefficients $A_{vc}^S$ and $B_{vc}^S$, in terms of which the Bethe-Salpeter equation can be expressed. With this aim in mind, if one takes the Fourier transformed BSE and assumes that the pole at $\Omega_S$ is isolated from the other poles in the frequency complex plane, the application of Jordan's lemma allows a

contour integration around the pole to be performed and the reaching of the equations

$$A^S_{vc}\psi_c(\mathbf{x}_1)\psi^*_v(\mathbf{x}_{1'})e^{-i\Omega_S t_1} = \sum_{v'c'}\int d33'44'G_1(1,3)G_1(3',1')i\Xi(3,4';3',4)\cdot \\ \cdot\left[A^S_{v'c'}\psi_{c'}(\mathbf{x}_4)\psi^*_{v'}(\mathbf{x}_{4'})e^{-i\Omega_S t_4} + B^S_{v'c'}\psi_{v'}(\mathbf{x}_4)\psi^*_{c'}(\mathbf{x}_{4'})e^{i\Omega_S t_4}\right] \quad (2.19)$$

and

$$B^S_{vc}\psi_v(\mathbf{x}_1)\psi^*_c(\mathbf{x}_{1'})e^{i\Omega_S t_1} = \sum_{v'c'}\int d33'44'G_1(1,3)G_1(3',1')i\Xi(3,4';3',4)\cdot \\ \cdot\left[A^S_{v'c'}\psi_{c'}(\mathbf{x}_4)\psi^*_{v'}(\mathbf{x}_{4'})e^{-i\Omega_S t_4} + B^S_{v'c'}\psi_{v'}(\mathbf{x}_4)\psi^*_{c'}(\mathbf{x}_{4'})e^{i\Omega_S t_4}\right], \quad (2.20)$$

for $\Omega_S > 0$ and $\Omega_S < 0$ respectively. Such writings are actually generalized eigenvalue problems with eigenvectors $A^S$ and $B^S$ and eigenvalues $\pm\Omega_S$: multiplying by $(E_c - E_v - \Omega_S)\psi^*_c(\mathbf{x}_1)\psi_v(\mathbf{x}_{1'})$ both sides of the first equation and by $(E_c - E_v + \Omega_S)\psi^*_c(\mathbf{x}_1)\psi_v(\mathbf{x}_{1'})$ the second one and then integrating over $x_1$ and $x_{1'}$ the orthonormality conditions yield to

$$(E_c - E_v)A^S_{vc} + \sum_{v'c'} K^{AA}_{vc,v'c'}(\Omega_S)A^S_{v'c'} + \sum_{v'c'} K^{AB}_{vc,v'c'}(\Omega_S)B^S_{v'c'} = \Omega_S A^S_{vc}, \quad (2.21)$$

$$\sum_{v'c'} K^{BA}_{vc,v'c'}(\Omega_S)A^S_{v'c'} + (E_c - E_v)B^S_{vc} + \sum_{v'c'} K^{BB}_{vc,v'c'}(\Omega_S)B^S_{v'c'} = -\Omega_S A^S_{vc}, \quad (2.22)$$

where

$$K^{AA}_{vc,v'c'}(\Omega_S) = i\int d3456\psi_v(\mathbf{x}_4)\psi^*_c(\mathbf{x}_3)\Xi(3,5;4,6)\psi^*_{v'}(\mathbf{x}_5)\psi_{c'}(\mathbf{x}_6), \quad (2.23)$$

$$K^{AB}_{vc,v'c'}(\Omega_S) = i\int d3456\psi_v(\mathbf{x}_4)\psi^*_c(\mathbf{x}_3)\Xi(3,5;4,6)\psi^*_{v'}(\mathbf{x}_6)\psi_{c'}(\mathbf{x}_5), \quad (2.24)$$

$$K^{BA}_{vc,v'c'}(\Omega_S) = i\int d3456\psi_v(\mathbf{x}_3)\psi^*_c(\mathbf{x}_4)\Xi(3,5;4,6)\psi^*_{v'}(\mathbf{x}_5)\psi_{c'}(\mathbf{x}_6), \quad (2.25)$$

and

$$K^{BB}_{vc,v'c'}(\Omega_S) = i\int d3456\psi_v(\mathbf{x}_3)\psi^*_c(\mathbf{x}_4)\Xi(3,5;4,6)\psi^*_{v'}(\mathbf{x}_6)\psi_{c'}(\mathbf{x}_5). \quad (2.26)$$

However, the off diagonal terms $K^{AB}$ and $K^{BA}$ were proven to have very little influence on the optical properties of a semiconductor [16]. Consideration of only diagonal terms permits the decoupling of the two equations which in this case have the same solutions apart from the sign of the eigenvalue. Henceforth we will keep only the eigenvalue problem giving positive solutions, i. e.

$$(E_c - E_v)A^S_{vc} + \sum_{v'c'} K^{AA}_{vc,v'c'}(\Omega_S)A^S_{v'c'} = \Omega_S A^S_{vc}. \quad (2.27)$$

This assumption can equivalently be formulated with the writing

$$|N,S\rangle = \sum_{v}^{hole}\sum_{c}^{elec} A_{vc}^{S}\,|vc\rangle\,, \tag{2.28}$$

known as *Tamm-Dancoff approximation*. In other terms, we assume an excitonic state to be a superposition of decoupled electron-hole states. It is essential to notice that the two particle interaction terms depend explicitly on the screened Coulomb interaction $W$. As a consequence, such quantity must be accurately evaluated for a solution of the Bethe-Salpeter equation (2.27) to be attained.

### 2.2.3 Application of GW approximation

In the present work the screened Coulomb interaction is computed within the $G_0W_0$ approximation presented in §1.4.3, and the form

$$\begin{aligned}\Xi(3,6;4,5) &= -i\hbar\delta(3,6)\delta(4,5)v(3,4) + i\hbar\delta(3,5)\delta(6,4)W(3^+,4) = \\ &= K_x(3,6;4,5) + K_d(3,6;4,5),\end{aligned} \tag{2.29}$$

is obtained under the assumption of $W$ constant with respect to the variation of the single-particle Green's function. The attractive electron-hole interaction responsible for the formation of bound states (excitons) lies in the direct contribution $K_d$ (involving $W$), while the exchange interaction term $K_x$ provides the details of the excitation spectrum, such as the splitting between spin-singlet and spin-triplet excitons. The matrix elements of $K$ expressed in the basis $|vc\rangle$ of electron-hole couples read

$$\langle vc|\,K_x^{AA}\,|v'c'\rangle = \int d\mathbf{x}d\mathbf{x}'\psi_c^*(\mathbf{x})\psi_v(\mathbf{x})v(\mathbf{r},\mathbf{r}')\psi_{c'}(\mathbf{x}')\psi_{v'}(\mathbf{x}') \tag{2.30}$$

and

$$\begin{aligned}\langle vc|\,K_d^{AA}(\Omega_S)\,|v'c'\rangle = \int d\mathbf{x}d\mathbf{x}'\psi_c^*(\mathbf{x})\psi_{c'}(\mathbf{x})\psi_v(\mathbf{x}')\psi_{v'}^*(\mathbf{x}')\frac{i}{2\pi}\int d\omega e^{-i\omega\delta}W(\mathbf{r},\mathbf{r}';\omega)\cdot \\ \cdot\left[\frac{1}{\Omega_S-\omega-(E_{c'}^{QP}-E_v^{QP})+i\delta}+\frac{1}{\Omega_S+\omega-(E_c^{QP}-E_v^{QP})+i\delta}\right].\end{aligned} \tag{2.31}$$

In the direct term the screened Coulomb interaction has bee Fourier transformed, with $\delta\to 0^+$. In semiconductor crystals however the differences $\Omega_S-(E_{c'}^{QP}-E_v^{QP})$ are much smaller than the energies $\omega$ controlling the dynamics of the screening. Thus, in such case a static version of the screened interaction can be considered, which implies the expression

$$\langle vc|\,K_d^{AA}(\Omega_S)\,|v'c'\rangle = -\int d\mathbf{x}d\mathbf{x}'\psi_c^*(\mathbf{x})\psi_{c'}(\mathbf{x})\psi_v(\mathbf{x}')\psi_{v'}^*(\mathbf{x}')W(\mathbf{r},\mathbf{r}';\omega=0). \tag{2.32}$$

The knowledge of the screened Coulomb interaction $W$, of the quasi-particle energies $E^{QP}$ and of the band structure is then sufficient to compute the excitonic energies $\Omega_S$. However, this process requires an elevated computation cost because of the high number of products necessary to evaluate all the matrix elements. One possible way to speed up the calculation is to reduce the number of states of the bases considered: such approach will be examined in the following chapter.

## 2.3 Longitudinal dielectric function in extended systems

Once the excitation energies are computed, we will need to compute a macroscopic quantity which must be experimentally obtainable: the absorption coefficient, defined as

$$\eta(\omega) = \frac{2\omega}{c}\sqrt{\frac{\sqrt{\varepsilon_1^2(\omega)+\varepsilon_2^2(\omega)}-\varepsilon_1(\omega)}{2}}. \tag{2.33}$$

The functions $\epsilon_1(\omega)$ and $\epsilon_2(\omega)$ are the real and imaginary part of the dielectric macroscopic function $\epsilon(\omega)$. We are now going to present a way to express the dielectric function in terms of the excitonic transitions in a complex system, following the procedure discussed in [20].

The basic idea is to derive the expressions for the power $\mathscr{P}(\mathbf{q},\omega)$ dissipated in the system under the effect of an external electric potential form a macroscopical and a quantum point of view, and set them to be equal. We assume the system to be subdued to an external small perturbation

$$U(\mathbf{r},t) = U_0 e^{i\mathbf{q}\cdot\mathbf{r}-i\omega t} + c.c. \tag{2.34}$$

where $U_0(\mathbf{q},\omega)$ is the amplitude and *c.c.* stands for the complex conjugate of the first addend. Limiting our treatment to an electric potential, we have $\phi = -eU$; consequently the application of the gradient with respect to $\mathbf{q}$ yields to the electric field

$$\mathbf{E}(\mathbf{r},t) = \frac{iU_0}{e}\mathbf{q}e^{i\mathbf{q}\cdot\mathbf{r}-i\omega t} + c.c.\ . \tag{2.35}$$

The probability of the occurrence of an excitation of the type $|N,0\rangle \to |N,S\rangle$ under a perturbation of amplitude $U_0$ is given by the Fermi Golden rule:

$$P_s(\mathbf{q},\omega) = 2\pi \left|\langle S| U_0 e^{i\mathbf{q}\cdot\mathbf{r}} |0\rangle\right|^2 \delta(\Omega_S - \omega) \tag{2.36}$$

with $\Omega_S$ energy of the excitation. The number of transitions with momentum $\mathbf{q}$ and frequency $\omega$ is $W(\mathbf{q},\omega) = \sum_S P_S(\mathbf{q},\omega)$, then the total power dissipated in a volume $V$ is

$$\mathscr{P}(\mathbf{q},\omega) = \omega W(\mathbf{q},\omega) = \omega 2\pi \sum_S \left|\langle S| U_0 e^{i\mathbf{q}\cdot\mathbf{r}} |0\rangle\right|^2 \delta(\Omega_S - \omega). \tag{2.37}$$

On the other hand, exploiting the definition of the conductibility function $\sigma$, the macroscopic electric current $\mathbf{J}$ induced by an electric field in an isotropic and homogeneous medium is equal to $\sigma\mathbf{E}$. The dissipated power is then

$$\mathscr{P}(\mathbf{q},\omega) = \int_V d^3\mathbf{r}\mathbf{J}\cdot\mathbf{E} = V\sigma(\mathbf{q},\omega)\left|\frac{iqU_0}{e}\right|^2 + c.c. = 2V\sigma_1(\mathbf{q},\omega)\left|\frac{qU_0}{e}\right|^2, \tag{2.38}$$

and the confrontation with eq. (2.37) provides the relation

$$\sigma_1(\mathbf{q},\omega) = \frac{e^2}{2q^2}\frac{\omega W(\mathbf{q},\omega)}{|U_0|^2 V}. \tag{2.39}$$

Recalling the definition (2.1) of the dielectric function, it is easy to obtain the equation

$$\frac{\partial(\varepsilon\mathbf{E})}{\partial t} = \frac{\partial\mathbf{E}}{\partial t} + 4\pi\sigma\mathbf{E}. \tag{2.40}$$

The Fourier transform of the electric field then leads to a relation between the dielectric function $\varepsilon$ and the conductivity $\sigma$:

$$\varepsilon(\mathbf{q},\omega) = 1 + \frac{4\pi}{\omega}i\sigma(\mathbf{q},\omega), \tag{2.41}$$

and as a consequence we finally obtain

$$\varepsilon_2(\mathbf{q},\omega) = \frac{4\pi}{\omega}i\sigma_1(\mathbf{q},\omega) = \frac{4\pi^2e^2}{q^2V}\sum_S \left|\langle S|\, e^{i\mathbf{q}\cdot\mathbf{r}}\,|0\rangle\right|^2 \delta(\Omega_S-\omega). \tag{2.42}$$

For the fact we are interested into the long wavelength limit, the limit $\mathbf{q}\to 0$ can be taken:

$$\varepsilon_2(\omega) = \lim_{\mathbf{q}\to 0}\frac{4\pi^2e^2}{q^2V}\sum_S |\langle S|\, i\mathbf{q}\cdot\mathbf{r}\,|0\rangle|^2\,\delta(\Omega_S-\omega) = -\frac{4\pi e^2}{V}\sum_S |\hat{q}\cdot\langle S|\,\mathbf{r}\,|0\rangle|^2\,\delta(\Omega_S-\omega). \tag{2.43}$$

The matrix element obtained can not be directly evaluated in the case of an extended system, because the action of the position operator $\mathbf{r}$ is not well defined. Thus, keeping in mind that $\Omega_S$ is the energy difference between the states $|0\rangle$ and $|S\rangle$, we rewrite it in the form

$$\langle S|\,\mathbf{r}\,|0\rangle = \frac{\langle S|\,\mathbf{r}\Omega_S\,|0\rangle}{\Omega_S} = \frac{\langle S|\,[\mathbf{r},H]\,|0\rangle}{\Omega_S} = \frac{\langle S|\,[\mathbf{r},\mathbf{p}^2]\,|0\rangle}{2m\Omega_S} + \frac{\langle S|\,[\mathbf{r},V_{ps}]\,|0\rangle}{\Omega_S}. \tag{2.44}$$

The last term is non-vanishing when a non-local pseudopotential is adopted. However, it was proven that its introduction does not affect greatly the spectrum but provides a 10% correction. In this work such term will be omitted, hence the imaginary part of

the dielectric function is assumed to be

$$\varepsilon_2(\omega) = -\frac{4\pi^2 e^2}{V} \sum_S \frac{|\hat{q} \cdot \langle S| \, i\mathbf{p} \, |0\rangle|^2}{m^2 \Omega_S^2} \delta(\Omega_S - \omega) = \frac{4\pi^2 e^2}{V m^2 \omega^2} \sum_S |\hat{q} \cdot \langle S| \, \mathbf{p} \, |0\rangle|^2 \, \delta(\Omega_S - \omega). \tag{2.45}$$

The real part can now be attained using the Kramers-Kronig relation

$$\varepsilon_1(\omega) = 1 + \frac{1}{\pi} \mathcal{P} \int_{-\infty}^{+\infty} d\omega' \frac{\varepsilon_2(\omega')}{\omega' - \omega} = 1 + \sum_S \frac{4\pi e^2}{V m^2 \Omega_S^2} |\hat{q} \cdot \langle S| \, \mathbf{p} \, |0\rangle|^2 \, \mathcal{P} \frac{1}{\Omega_S - \omega}. \tag{2.46}$$

In conclusion, starting from the identity

$$\lim_{\eta \to 0} \frac{1}{\omega - \Omega_S - i\eta} = \mathcal{P} \frac{1}{\Omega_S - \omega} + i\pi \delta(\omega - \Omega_S) \tag{2.47}$$

it is straightforward to see that the multiplication by $\frac{4\pi e^2}{V m^2}$ and the summation over $S$ on both sides, along with equations (4.2.2), (2.46), yields to

$$\varepsilon(\omega) = \varepsilon_1(\omega) + i\varepsilon_2(\omega) = 1 + \sum_S \frac{4\pi e^2}{V m^2 \Omega_S^2} \frac{|\hat{q} \cdot \langle S| \, \mathbf{p} \, |0\rangle|^2}{\Omega_S - \omega - i\eta}. \tag{2.48}$$

Although the expressions just derived are valid for generic transitions $|0\rangle \to |S\rangle$, in the present work the case of excitionic ones will be considered. The GW and BSE formalisms will be exploited to compute the matrix elements and the excitation energies $\Omega_S$ and then to evaluate $\varepsilon$. Nevertheless, the number of excited states to be considered in order to obtain a converged spectrum using a direct implementation of eq. (2.48) will be proven to be too elevated: a more efficient method will be therefore necessary.

# Chapter 3

# Implementation techniques

This chapter is devoted to the computational methods adopted to perform the calculations. The programs used are all included in the `Quantum Espresso` suite of ab-initio codes for electronic structure computations [19]. DFT methods are implemented in the `pw` code, the GW approximation in the `GWL` code.
The newly developed routines for both the solution of BSE and the computation of optical spectra are programmed within `QE` distribution as post-processing codes. All matrix multiplications are efficiently performed via the LAPACK [25] and BLAS [26] libraries and MPI parallelization is used.

## 3.1 Plane waves and grid methods for the solution of Kohn-Sham equations

In this section the method employed for the solution of Kohn-Sham equations will be presented.
The starting point of our treatment is the independent-particle Schrödinger equation (1.8). Our approach is to expand the wave functions in terms of orthonormalized plane-waves:

$$\psi_i(\mathbf{r}) = \sum_{\mathbf{k}} c_{i,\mathbf{k}} |\mathbf{k}\rangle \qquad \text{with} \qquad |\mathbf{k}\rangle = \frac{1}{\sqrt{\Omega}} e^{i\mathbf{k}\cdot\mathbf{r}}. \tag{3.1}$$

The effective Hamiltonian can then be expressed in such basis:

$$\langle \mathbf{k}'| \hat{H}_{eff} |\mathbf{k}\rangle = \frac{1}{2}|k|^2 \delta_{\mathbf{k},\mathbf{k}'} + \sum_m V_{eff}(\mathbf{G}_m)\delta_{\mathbf{k}-\mathbf{k}',\mathbf{G}_m}. \tag{3.2}$$

In the last passage the periodicity of the potential was exploited; in addition, reciprocal lattice vectors were denoted with $\mathbf{G}_m$ and the Fourier components of the potential are

$$V_{eff}(\mathbf{G}) = \frac{1}{\Omega_{cell}} \int_{\Omega_{cell}} d^3r V_{eff}(\mathbf{r}) e^{-i\mathbf{G}\cdot\mathbf{r}} \tag{3.3}$$

where $\Omega_{cell}$ is the volume of the primitive cell. Inserting such expressions with an appropriate redefinition of the wavevectors in eq. (1.8) we find the basic Schrödinger's equations for a periodic system

$$\sum_{m'} H_{m,m'}(\mathbf{k}) c_{i,m'}(\mathbf{k}) = \epsilon_i(\mathbf{k}) c_{i,m}(\mathbf{k}) \tag{3.4}$$

where we defined

$$H_{m,m'}(\mathbf{k}) \equiv \frac{1}{2}|\mathbf{k}+\mathbf{G}_m|^2 \delta_{m,m'} + V_{eff}(\mathbf{G}_m - \mathbf{G}_{m'}). \tag{3.5}$$

Each Fourier component of the solutions of such equations can also be written in the form

$$\psi_{i,\mathbf{k}}(\mathbf{r}) = \sum_m c_{i,m}(\mathbf{k}) \frac{e^{i(\mathbf{k}+\mathbf{G}_m)\cdot\mathbf{r}}}{\sqrt{N_{cell}\Omega_{cell}}} = \frac{e^{i\mathbf{k}\cdot\mathbf{r}}}{\sqrt{N_{cell}}} u_{i,\mathbf{k}}(\mathbf{r}) \tag{3.6}$$

where

$$u_{i,\mathbf{k}}(\mathbf{r}) = \sum_m c_{i,m}(\mathbf{k}) \frac{e^{i\mathbf{G}_m\cdot\mathbf{r}}}{\Omega_{cell}} \tag{3.7}$$

and $\Omega_{cell} = \Omega/N_{cell}$. The decomposition (3.6) is known as the Bloch theorem: the Fourier components of a wave function are written in terms of a function $u_{i,\mathbf{k}}$ with the same periodicity of the crystal and of a plane wave with $\mathbf{k}$ in the first Brillouin zone (BZ). As a consequence, the integrations over $\mathbf{k}$ necessary to compute several physical quantities can be performed on the volume in the reciprocal space corresponding to just the first Brillouin zone.
In addition, such volume can be further reduced in the presence of point symmetries. In other terms, if there is some combination of rotations, inversions, reflections $R_n$ and translations $\mathbf{t}_n$ that leaves the system invariant, $R_n g(\mathbf{r}) = g(R_n\mathbf{r} + \mathbf{t}_n)$ with $g$ any property of the system, then one has additional costraints on the wave functions. Integrations over the BZ can then be replaced with integrations over the so-called irreducible Brillouin zone (IBZ), greatly simplifying the calculations.

Let us take into consideration the evaluation of the density $n(\mathbf{r})$, which can be expressed in the form

$$n(\mathbf{r}) = \frac{1}{N_k} \sum_{i,\mathbf{k}} f(\epsilon_{i,\mathbf{k}}) n_{i,\mathbf{k}}(\mathbf{r}); \tag{3.8}$$

$f(\epsilon_{i,\mathbf{k}})$ is some function of the single-particle eigenvalues, while

$$n_{i,\mathbf{k}}(\mathbf{r}) = |\psi_{i,\mathbf{k}}(\mathbf{r})|^2 = \frac{1}{\Omega} \sum_{m,m'} c^*_{i,m}(\mathbf{k}) c_{i,m'}(\mathbf{k}) e^{-i(\mathbf{G}_m - \mathbf{G}_{m'})\cdot\mathbf{r}}. \tag{3.9}$$

The calculation of the latter defined coefficients requires the double summation over plane waves, with a computational cost equal to the square of the total number of plane waves, $N_G^2$. However, the same result is attained in real space with a number of operations corresponding to the number of Bravais vectors, $N_R$. It is thus convenient

to express all quantities in real space via a Fourier transformation using FFT methods: such process requires $N \log N$ operations ($N_R = N = N_G$) and a regular piped-like grid with plane waves satisfying the condition $|\mathbf{k}+\mathbf{G}|^2/2 < E_{cutoff}$ with $E_{cutoff}$ user defined cutoff energy. Even if the number of grid points required for this method is one order of magnitude bigger, the approach is proven to still be faster in the case of extended systems.

## 3.2 Lanczos-chain algorithm

The Lanzcos-chain algorithm provides an efficient method to compute a tridiagonal matrix $T$ which is similar to an hermitian $n \times n$ matrix $A$. The importance of such operation lies in the fact that the diagonalization of the matrix $T$ can be performed via much faster methods than the one of $A$. As a consequence, if we tridiagonalize a matrix before we diagonalize it we considerably reduce the computational cost of the process. Since this approach will be adopted for both the calculation of the optical spectrum and the implementation of the $G_0W_0$ approximation, its main features will be here presented.
The first step of the algorithm is the selection of a normalized vector $|P\rangle \equiv |1\rangle$ which constitutes the starting point for the construction of the tridiagonal symmetrical $n \times n$ matrix $T$; its diagonal elements will be denoted with $a_i$ ($i = 1, \cdots, n$), while the off diagonal ones with $b_j$ ($j = 1, \cdots, n-1$). Depending on the context, one can choose $|P\rangle$ to be either of a particular form or a random normalized vector. The first coefficient is then set to be $a_1 = \langle 1| A |1\rangle$, and the second element of the base on which the matrix will be represented is constructed as

$$|2\rangle = \frac{A|1\rangle - a_1|1\rangle}{b_1} \qquad \text{with} \qquad b_1 = |A|1\rangle - a_1|1\rangle|\,. \tag{3.10}$$

The orthonormalization of the so-defined vectors $|1\rangle$ and $|2\rangle$ is easily proved, and the second diagonal coefficient is given by $a_2 = \langle 2| A |2\rangle$. Henceforth, the remaining vectors are built through the recursive relation

$$|i+1\rangle = \frac{A|i\rangle - a_i|i\rangle - b_{i-1}|i-1\rangle}{b_i} \tag{3.11}$$

where the coefficients are

$$a_i = \langle i| A |i\rangle \qquad \text{and} \qquad b_i = |A|i\rangle - a_i|i\rangle - b_{i-1}|i-1\rangle|. \tag{3.12}$$

After $n$ iterations the matrix

$$T = \begin{pmatrix} a_1 & b_1 & 0 & \dots & \dots & 0 \\ b_1 & a_2 & b_2 & 0 & \dots & \vdots \\ 0 & b_2 & \ddots & \ddots & \ddots & \vdots \\ \vdots & 0 & \ddots & \ddots & b_{n-2} & 0 \\ \vdots & \vdots & \ddots & b_{n-2} & a_{n-1} & b_{n-1} \\ 0 & \dots & \dots & 0 & b_{n-1} & a_n \end{pmatrix} \tag{3.13}$$

is then constructed, along with the orhonormal basis $\{|i\rangle\}_{i=1,\dots,n}$.

### 3.2.1 Haydoch recursive method for optical spectra

An extended version of the Lanczos-chain method can be applied in order to evaluate matrix elements of the form

$$I = \langle P| \frac{1}{\hat{H} - \omega - i\eta} |P\rangle , \tag{3.14}$$

which are essential to the computation of the optical spectrum. The equation (2.48) for the dielectric function can indeed be cast in a similar form. Exploiting the orthonormality of the basis $\{|S\rangle\}$ eq. (4.2.2) can be rewritten as

$$\begin{aligned} \varepsilon_2(\omega) &= \sum_S \frac{4\pi^2 e^2}{V m^2 \omega^2} \Im \langle 0| \hat{q} \cdot \mathbf{p} |S\rangle \langle S| \hat{q} \cdot \mathbf{p} |0\rangle \delta(\Omega_S - \omega) = \\ &= \frac{4\pi^2 e^2}{V m^2} \Im \left[ \langle 0| \frac{\hat{q} \cdot \mathbf{p}}{\omega} \frac{1}{\hat{H} - \omega - i\eta} \frac{\hat{q} \cdot \mathbf{p}}{\omega} |0\rangle \right]. \end{aligned} \tag{3.15}$$

It is then clear that in this case the starting vector of the Lanczos approach is

$$|P\rangle = \frac{\hat{q} \cdot \mathbf{p}}{\omega} |0\rangle = \sum_S \langle S| \frac{\hat{q} \cdot \mathbf{p}}{\omega} |0\rangle |S\rangle , \tag{3.16}$$

where $\{|S\rangle\}$ is a complete basis. We notice that the expansion elements in such basis are exactly of the same form of the one appearing in eq (4.2.2).
The so called Haydoch recursive method consists in the use of the coefficients found through the Lanzcos chain algorithm to build the expression (3.14) as a continued fraction. As previously enlightened, the Lanczos approach provides an orthonormal basis made of the vectors $|i\rangle$ on which the Hamiltonian operator $\hat{H}$ has a tridiagonal form $H$. This fact, together with the introduction of the notation $z \equiv \omega + i\eta$, implies the validity of the writing

$$\sum_k \langle i| (H - z) |k\rangle \langle k| (H - z)^{-1} |j\rangle = \delta_{ij}. \tag{3.17}$$

Furthermore, the choice $j = 1$ and the definition $X_i = \langle i| (H - z)^{-1} |1\rangle$ yield to

$$\sum_k (z - H)_{ik} X_k = \delta_{k1}, \tag{3.18}$$

which is nothing but a linear system of equations for $X_i$, $i = 1, \ldots$. Let us note that the quantity $X_1$ actually coincides with the matrix element (3.14) that we are trying to evaluate. Thus, denoting with $B$ a matrix identical to $(z - H)$ apart from having as first column the vector $(1\ 0 \cdots\ 0)^T$, it is straightforward to show that

$$X_1 = \frac{\det B}{\det (H - z)}. \tag{3.19}$$

Moreover, if $D_i$ is the matrix $(z - H)$ deprived of the first $i$ rows and columns, it easy to see that

$$\det (H - z) = (a_1 - z) \det D_1 - b_1^2 \det D_2 \tag{3.20}$$

and $\det B = \det D_1$. Consequently, we obtain

$$I \equiv X_1 = \frac{\det D_1}{(a_1 - z) \det D_1 - b_1^2 \det D_2} = \frac{1}{(a_1 - z) - b_1^2 \frac{\det D_2}{\det D_1}}. \tag{3.21}$$

Henceforth, a continued fraction can be attained iteratively using the relation

$$\det D_i = (a_{i+1} - z) \det D_{i+1} - b_{i+1} \det D_{i+2}, \tag{3.22}$$

namely

$$I = \cfrac{1}{(a_1 - z) - \cfrac{b_1^2}{(a_2 - z) - \cfrac{b_2^2}{a_3 - z - \ldots}}}. \tag{3.23}$$

We note that the frequency appears in the continued fraction as a mere parameter, so that the whole procedure must not be repeated for each energy: the estimation of $I$ for one frequency yields its value for all the others. This feature makes the Haydoch recursive method particularly suitable and efficient for the computation of spectra.

**Algorithm 1** Haydoch recursive method

Construction of $|P\rangle$
Lanczos tridiagonalization of $\hat{H}$
Construction of the continued fraction

In practice, one has to truncate the continued fraction since only a finite number of coefficients is available. Our approach is to set the $n$-th off-diagonal coefficient, $b_n$, to zero, where $n$ is the number of iterations. Clearly, the method will be the most accurate the highest number of iterations is selected. As later explained, we find converged spectra for a number of iterations that ranges between 200 and 400.

## 3.3 Efficient $G_0W_0$-Lanczos method

As already mentioned, GW approximation provides more accurate results than DFT, but it has a much higher computational cost: the bases on which operators are expanded are composed by a large number of elements, so the evaluation of products between operators and the matrix elements is very computationally demanding. However, many of the Kohn-Sham states over which the sums are computed are actually empty and the dimension of the bases can be diminished taking only the vectors corresponding to the largest eigenvalues. In this work the Lanczos method is combined with the $G_0W_0$ approximation in order to obtain an optimal basis for the irreducible polarizability $P$. The same basis can then be adopted for the representation of the self energy. The approach here described is implemented in the `GWL` code ([21],[22]), included in the `QUANTUM ESPRESSO` suite [19].

Let us consider the zero-time irreducible polarizability

$$P(\mathbf{r},\mathbf{r}';t=0)=\frac{1}{2}\sum_{vc}\left[\psi_v(\mathbf{r})\psi_c^*(\mathbf{r})\psi_v^*(\mathbf{r}')\psi_c(\mathbf{r}')+\psi_c^*(\mathbf{r}')\psi_v(\mathbf{r}')\psi_c(\mathbf{r})\psi_v^*(\mathbf{r})\right]. \tag{3.24}$$

Our objective is to find a basis $\{|\Phi_\mu\rangle\}$ of eigenvectors corresponding to the largest eigenvalues $p_\mu$ of $\tilde{P}$. This can be accomplished via a singular value decomposition (SDV) of the basis $\psi_v(\mathbf{r})\psi_c^*(\mathbf{r})\equiv\langle\mathbf{r}|\psi_v\psi_c\rangle$. This method allows the writing of an $m\times n$ matrix $M$ as the product $U\cdot\Sigma\cdot V^*$, where $\Sigma$ is a diagonal $m\times n$ matrix and $U$ and $V$ are unitary matrices of dimensions $m\times m$ and $n\times n$ respectively. Then, the matrix $Q_{\alpha\beta}\equiv Q_{vc,v'c'}=\langle\psi_v\psi_c|\psi_{v'}\psi_{c'}\rangle$ can be written as

$$\sum_\beta Q_{\alpha\beta}|q_\beta^\mu\}=q_\mu|q_\alpha^\mu\} \tag{3.25}$$

with eigenvectors $|q_\alpha^\mu\}$ and eigenvalues $q_\mu$. As a consequence the definition of the orthonormalized vectors

$$|\Phi_\mu\rangle=\sum_\alpha\frac{1}{\sqrt{q_\mu}}|q_\alpha^\mu\}\,|\psi_{v_\alpha}\psi_{c_\alpha}\rangle \tag{3.26}$$

is possible. In order to improve the efficiency of the SVD an energy cutoff $E^*$ is set, and only conduction states with energies below $E^*$ will be considered. In other terms, we select only plane-waves satisfying the condition $\frac{1}{2}|\mathbf{G}|^2\leq E^*$ and then construct the augmented plane-waves $\{\tilde{\mathbf{G}}\}$ through a projection onto the conduction states manifold:

$$|\tilde{\mathbf{G}}\rangle=\left(1-\sum_v|\psi_v\rangle\langle\psi_v|\right)|\mathbf{G}\rangle. \tag{3.27}$$

The completeness of the Hilbert space spanned by both valence and conduction states was exploited. The zero-time polarizability operator can thus be written as

$$\tilde{P}(t=0)=\sum_{vc}|\psi_v\tilde{\mathbf{G}}_c\rangle\langle\psi_v\tilde{\mathbf{G}}_c|, \tag{3.28}$$

where the $\{\tilde{\mathbf{G}}_c\}$ basis is composed by nothing but the orthonormalized $\tilde{\mathbf{G}}$s.
At this rate, it is convenient to express the valence states in terms of localized Wannier functions [27]. If a Bloch orbital is denoted with $\psi_{\mathbf{k}}(\mathbf{r}) = e^{i\mathbf{k}\cdot\mathbf{r}}u_{\mathbf{k}}(\mathbf{r})$, the *Wannier function* corresponding to the Bravais lattice $\mathbf{R}$ is defined as

$$w_{\mathbf{R}}(\mathbf{r}) = \frac{1}{\sqrt{N}} e^{i\theta(\mathbf{k})} e^{i\mathbf{k}\cdot\mathbf{R}} \psi_{\mathbf{k}}(\mathbf{r}), \tag{3.29}$$

where $N$ is the number of primitive cells and $\mathbf{k}$ is taken in the first Brillouin zone. It is known that the Bloch states are invariant under unitary transformations of the form $e^{i\theta(\mathbf{k})}$ for any real $\theta(\mathbf{k})$. Nevertheless, the choice of the phase greatly influences the Wannier functions: choosing suitably the function $\theta(\mathbf{k})$ is indeed crucial to obtain simple Wannier functions. In the present work the maximally localized Wannier functions are adopted. Moreover, Bloch states can be unitarily transformed into Wannier functions, thus the operator

$$\tilde{P}(t=0) = \sum_{v,c} \left| w_v \tilde{\mathbf{G}}_c \right\rangle \left\langle w_v \tilde{\mathbf{G}}_c \right| \tag{3.30}$$

is attained. Since the basis adopted is not orthonormalized, a modified Gram-Schmidt algorithm is employed to construct a set of orthonormalized vectors $|f_\alpha\rangle$, with a user defined threshold parameter $s$: the direct diagonalization of the overlap matrix $\left| w_v \tilde{\mathbf{G}}_c \right\rangle$ is this way avoided and an adequate selection of $s$ produces a number of states $|f_\alpha\rangle$ much smaller than $N_c N_v$. The matrix elements

$$\tilde{P}_{\alpha\beta}(t=0) = \sum_{v,c} \langle f_\alpha | w_v \tilde{\mathbf{G}}_c \rangle \langle w_v \tilde{\mathbf{G}}_c | f_\beta \rangle \tag{3.31}$$

are then computed and given the equation

$$\sum_\beta \tilde{P}_{\alpha\beta} |p^\mu_\beta\} = p_\mu |p^\mu_\alpha\} \tag{3.32}$$

the optimal polarizability basis is eventually built:

$$|\Phi_\mu\rangle = \sum_\alpha |p^\mu_\alpha\} \, |f_\alpha\rangle \, . \tag{3.33}$$

The notation $|p^\mu_\alpha\}$ was adopted in order to remind we are dealing with eigenvectors different from $|f_\alpha\rangle$. The method is naturally extended to the spin-polarized case, computing separately the bases $\{w^\sigma_v \tilde{\mathbf{G}}^\sigma_c\}$ for $\sigma = \uparrow, \downarrow$ and considering union of the two bases for the construction of the operator (3.31) and the basis (3.33).

### 3.3.1 Irreducible dynamical polarizability and self energy correction

We are now going to express the quantities of interest for the computation in the optimal basis $|\Phi_\mu\rangle$ just derived, with $N_P$ elements. For the spin-unpolarized case the irreducible dynamical polarizability at imaginary frequency can be written as

$$P(\mathbf{r},\mathbf{r}';i\omega) = -4\Re\left[\sum_{vc}\frac{\psi_v(\mathbf{r})\psi_c(\mathbf{r})\psi_v(\mathbf{r}')\psi_c(\mathbf{r}')}{\epsilon_c-\epsilon_v+i\omega}\right]. \tag{3.34}$$

Setting by definition $\langle r|\psi_v\Phi_\nu\rangle = \psi_v(\mathbf{r})\Phi_\nu(\mathbf{r})$ its expansion coefficients on the optimal basis $|\Phi_\mu\rangle$ are

$$P_{\mu\nu}(i\omega) = -4\Re\left[\sum_{vc}\int d^3\mathbf{r}d^3\mathbf{r}^3\Phi_\mu(\mathbf{r})\frac{\psi_v(\mathbf{r})\psi_c(\mathbf{r})\psi_v(\mathbf{r}')\psi_c(\mathbf{r}')}{\epsilon_c-\epsilon_v+i\omega}\Phi_\nu(\mathbf{r}')\right] = \tag{3.35}$$

$$= -4\Re\left[\sum_{v}\langle\psi_v\Phi_\mu|\,\hat{P}_c\frac{1}{\hat{H}-\epsilon_v+i\omega}\hat{P}_c\,|\psi_v\Phi_\mu\rangle\right]. \tag{3.36}$$

In the last passage the projection onto the conduction manifold was performed, and the final form was recovered exploiting the conduction projector property $\sum_c|\psi_c\rangle\langle\psi_c| = \hat{P}_c \equiv \hat{P}_c^2$. Note that the knowledge of the valence states is sufficient to the application of the projector onto the conduction manifold since $\hat{P}_c = 1-\hat{P}_v$. In order to further reduce the number $N_vN_P$ of inversion operations necessary for the computation, the approximation

$$\hat{P}_c\,|\psi_v\Phi_\mu\rangle \approx \sum_\alpha\langle t_\alpha|\psi_v\Phi_\mu\rangle\,|t_\alpha\rangle = \sum_\alpha T_{\alpha,v\mu}\,|t_\alpha\rangle \tag{3.37}$$

is adopted. The number $N_t$ of $t_\alpha$ vectors is user-defined and must be much smaller than $N_vN_P$. If the calculation is performed using Wannier functions instead of Kohn-Sham states $N_t$ can be proven to be almost independent from the size of the system. Finally we find

$$P_{\mu\nu}(i\omega) = -4\Re\sum_{v\alpha\beta}T^*_{\alpha,v\mu}T_{\beta,v\nu}\,\langle t_\alpha|\,\frac{1}{\hat{H}-\epsilon_v+i\omega}\,|t_\beta\rangle\,. \tag{3.38}$$

Since the expression recovered is analogous to eq. (3.14), the Lanczos method can be applied in order to further improve computational efficiency. Once the $P_{\mu\nu}$ is evaluated, also the reducible dynamical polarizability $\Pi(\mathbf{r},\mathbf{r}';i\omega)$ can be expanded in the optimal basis $\{\Phi_\mu\}$, with coefficients:

$$\Pi_{\mu\nu}(i\omega) = \left[P(i\omega)[1-vP(i\omega)]^{-1}\right]_{\mu\nu} \tag{3.39}$$

where

$$v_{\mu\nu} = \int d^3\mathbf{r}d^3\mathbf{r}'\,\langle\Phi_\mu|\,v(\mathbf{r},\mathbf{r}')\,|\Phi_\nu\rangle\,. \tag{3.40}$$

An analogous procedure can be performed to obtain an expression of the self energy in the same basis.

Both the polarization and the self-energy have been computed on the imaginary energy axis and then analytically continued. In this way they are represented by much smoother functions which still contain all the relevant information, and their products are of much simpler evaluation. The convenience of this procedure is supported by the fact Fast Fourier Transforms (FFTs) make the mapping between time (space) and momentum (energy) very efficient.

## 3.4 Solution of Bethe-Salpeter equation

To conclude this chapter, the method employed for the solution of the Bethe-Salpeter equation is presented.
The goal is to achieve an approach that allows the solving to be the most efficient possible, still maintaining a good level of accuracy. The main computational challenge lies in the dimension of the basis in which each excited state is expanded, because of the magnitude of both the numbers of KS states and of points of the grid with which the IBZ is represented. This implies that an enormous number of operations is needed for the evaluation of each matrix element.

Since each wave function is to be evaluated for every value of $\mathbf{k}$ in the first Brillouin zone, in theory a dense grid is in order. However, it is possible to extract detailed information on electronic structure for an arbitrary wave vector $\mathbf{k}$; an optimal basis spanning the IBZ is constructed and exploited to attain a k-dependent Hamiltonian. The wave functions are calculated on a uniform grid in reciprocal lattice space which may be characterized by the three integers $n_1 \times n_2 \times n_3$ whatever the lattice symmetry is. Interpolation techniques are then employed to extend the results to the rest of the Brillouin Zone. Such procedure is originally due to Shirley [28], later generalized in [29].

### 3.4.1 Optimal bases

As already explained, each excitonic state $|S\rangle$ is individuated by the coefficients $A^S_{vc}$ and within the Tamm-Dancoff approximation its wave function can be expressed as

$$\chi^S_{\mathbf{k}}(\mathbf{r}) = \sum_{vc} A^S_{vc} \Psi_{\mathbf{k}vc}(\mathbf{r}) \equiv \sum_{vc} A^S_{vc} \psi^*_{\mathbf{k}v}(\mathbf{r}) \psi_{\mathbf{k}c}(\mathbf{r}). \tag{3.41}$$

Each single particle wave function is further decomposed into a plane wave and a part which has the same period of the crystal lattice, according to Bloch theorem:

$$\psi_{\mathbf{k}\lambda}(\mathbf{r}) = e^{i\mathbf{k}\cdot\mathbf{r}} u_{\mathbf{k}\lambda}(\mathbf{r}) \tag{3.42}$$

for any $\lambda = v, c$. The total number of elements of the basis $u_{\mathbf{k}\lambda}$ is the product of the number of (both conduction and valence) states and the number of k-points considered.

It is easy to note that such number will grow considerably along with the size of the system, so the solving becomes the slower the biggest the system is. It is then natural to look for a way of reducing the basis elements taking into account only the ones that are the most relevant for the calculation. However, it is as well important to check whether the reduced basis leads to converged results or too many information were lost in the basis elements selection process.
In order to reduce the computational costs, it is convenient to adopt an optimal basis $\{|e_i\rangle\}$ for the representation of all the wave functions of the type $u_{\mathbf{k}\lambda}(\mathbf{r})$ with $\lambda = v, c$ for all the values of $\mathbf{k}$.
The set of vectors to be selected must be orthonormal and must contain all the essential knowledge. The construction of such basis is made by applying a modified Gram-Schmidt algorithm in which only the most relevant components of the basis are selected as follows. Starting from the complete plane wave basis for a certain value of $\mathbf{k}$, each of the basis vectors relative to the other $\mathbf{k}$s is deprived of its projection onto the space spanned by the already selected basis vectors. If the resulting vector has a modulus bigger than a certain user defined threshold $s_{pw}$ it is normalized and thus added to the basis, else it is discarded.

**Algorithm 2** Modified Gram-Schmidt, I

```
all basis elements for one k in the new basis
for all v, c, k do
  |v⟩ → |v⟩ − Σ_i ⟨e_i|v⟩ |e_i⟩
  if ⟨v|v⟩ ≥ s_pw then
    normalize |v⟩
    add |v⟩ to e_i basis
  end if
end for
```

Each element of the periodic part of the wave function basis can thus be expressed as a linear combination of elements of the newly found basis as

$$|u_{\mathbf{k}\lambda}\rangle = \sum_i \langle e_i|u_{\mathbf{k}\lambda}\rangle\,|e_i\rangle \equiv \sum_i E^{\mathbf{k}}_{i\lambda}\,|e_i\rangle\,, \tag{3.43}$$

and all the terms can be evaluated with respect to such vectors.
However, let us note that all the wave functions appearing in the two-particle interaction terms are always paired in products of the type $U_{\mathbf{k}\mu\nu}(\mathbf{r}) = u^*_{\mathbf{k}\mu}(\mathbf{r})u_{\mathbf{k}\nu}(\mathbf{r})$, with $\mu, \nu = v, c$. Moreover, it is logical to presume that not all of these products significantly contribute to the final result. It is thus convenient to introduce a second optimal basis, $\{|\mathcal{E}_\alpha\rangle\}$, for products between first optimal basis vectors.
Every product of the form $e^*_i e_j$ is considered for the construction of this second basis. For each fixed value of the index $i$ all the products with $j \leq i$ are computed. The approach is then very similar to the Gram-Schmidt above discussed: each product is normalized and added to the new basis only if its modulus is bigger than a user-defined threshold value $s_{prod}$.

**Algorithm 3** Modified Gram-Schmidt, II

**for** $i$ **do**
  **for** $j \leq i$ **do**
    $prod = e_i^* e_j$
    **if** $|prod| \geq s_{prod}$ **then**
      normalize $prod$
      add $prod$ to $\mathcal{E}_\alpha$ basis
    **end if**
  **end for**
**end for**

Henceforth, we attain the writing

$$|U_{\mathbf{k}vc}\rangle = |u^*_{\mathbf{k}v} u_{\mathbf{k}c}\rangle = \sum_{ij} E^{\mathbf{k}\,*}_{iv} E^{\mathbf{k}}_{jc} |e^*_i e_j\rangle = \sum_{ij\alpha} E^{\mathbf{k}\,*}_{iv} E^{\mathbf{k}}_{jc} F^{\alpha}_{ij} |\mathcal{E}_\alpha\rangle \equiv \sum_{\alpha} J^{\mathbf{k}}_{\alpha,vc} |\mathcal{E}_\alpha\rangle \,. \quad (3.44)$$

The matrix elements linking the old product basis with the new one were denoted with $F^{\alpha}_{ij} = \langle \mathcal{E}_\alpha | e^*_i e_j \rangle$. We also set for convenience $J^{\mathbf{k}}_{\alpha,vc} \equiv E^{\mathbf{k}\,*}_{iv} E^{\mathbf{k}}_{jc} F^{\alpha}_{ij}$. The importance of the construction of this latter basis increases with the number of elements of the basis $|e_i\rangle$, say $n_e$: the number of vectors of the products basis, $n_{\mathcal{E}}$, scales linearly with $n_e$ instead of its square when a threshold is introduced. To prove this, we note that in the absence of a threshold we have $n_{\mathcal{E}} \equiv n^0_{\mathcal{E}} = (n_e)^2$, while in the presence of a threshold $n_{\mathcal{E}} \equiv n^t_{\mathcal{E}} = a n_e$ with $a < n_e$ integer. Thus, if $n_e$ changes of a factor $L$, say $n'_e = n_e L$ we obtain $n^{0\,\prime}_{\mathcal{E}} = (n_e L)^2$ and $n^{t\,\prime}_{\mathcal{E}} = a L n_e$: the announced scaling property is demonstrated. These bases are not only employed in the evaluation of the BSE eigenstates, but also in the computation of the spectrum. The fundamental quantities to be estimated for that purpose are the matrix elements

$$\langle S | \, \mathbf{p} \, | 0 \rangle = \sum_{vc\mathbf{k}} A^{\mathbf{k}\,*}_{vc} \, \langle vc\mathbf{k} | \, \mathbf{p} \, | 0 \rangle = \sum_{vc\mathbf{k}} A^{\mathbf{k}\,*}_{vc} \, \langle c\mathbf{k} | \, \mathbf{p} \, | v\mathbf{k} \rangle \,. \quad (3.45)$$

Precisely, the matrix elements must be estimated using the relation

$$\langle v | \, \mathbf{p} \, | c \rangle^{[QP]} = \frac{E^{QP}_c - E^{QP}_v}{E^{LDA}_c - E^{LDA}_v} \, \langle v | \, \mathbf{p} \, | c \rangle^{[LDA]} \,, \quad (3.46)$$

as pointed out by Levine and Allan [18]. The exploitation of the optimal basis expansion coefficients allows the matrix elements to be cast in the form

$$\langle c\mathbf{k} | \, \mathbf{p} \, | v\mathbf{k} \rangle = \sum_{ij} E^{\mathbf{k}\,*}_{ic} E^{\mathbf{k}}_{jv} \, \langle e_i | \, \mathbf{p} \, | e_j \rangle \,. \quad (3.47)$$

Since the optimal bases do not change once the physical system is selected, it is convenient to compute them separately from the rest of the BSE solution saving the information on disk. This way different calculations on the same system will be performed much faster. In an analogous way, the expansion coefficients $E^{\mathbf{k}}_{ic}$, $E^{\mathbf{k}}_{iv}$, $F^{\alpha}_{ij}$ and

$J^{\mathbf{k}}_{\alpha,vc}$ are preliminarily evaluated, before the actual solution of BSE takes place.

### 3.4.2 Treating of the interaction kernel

The eigenvalue equation (2.27) is considered at different degree of approximation:

1. RPA: the electron-hole interaction kernel $\Xi$ is set to zero.

2. TD-H: the exchange kernel term (2.30) is added, and the so called time-dependent-Hartree approximation is recovered.

3. TD-HF: the direct kernel term is preliminarily computed using the bare Coulomb interaction $v$ instead of the screened interaction $W$, namely

$$\langle \mathbf{k}vc|\, K^{d,\text{bare}}\, |\mathbf{k}'v'c'\rangle = -\int d\mathbf{r}d\mathbf{r}'\psi^*_{\mathbf{k}c}(\mathbf{r})\psi_{\mathbf{k}'c'}(\mathbf{r})v(\mathbf{r},\mathbf{r}')\psi_{\mathbf{k}v}(\mathbf{r}')\psi^*_{\mathbf{k}'v'}(\mathbf{r}'); \quad (3.48)$$

   its addition leads to the time-dependent-Hartree-Fock approximation.

4. BSE: the proper direct term is considered and the Bethe-Salpeter equation is attained.

This division allows the effect of every single term to be separately examined.

Let us now see how to express the kernel terms (3.48) and (2.32) in the above defined bases. For the exchange kernel term with the bare interaction the exploitation of the completeness relations of the different bases yields to

$$\begin{aligned} K^x_{\mathbf{k}vc,\mathbf{k}'v'c'} \equiv \langle \mathbf{k}vc|\, K^x\, |\mathbf{k}'v'c'\rangle &= \int d\mathbf{r}d\mathbf{r}' u^*_{\mathbf{k}c}(\mathbf{r})u_{\mathbf{k}v}(\mathbf{r})v(\mathbf{r},\mathbf{r}')u^*_{\mathbf{k}'v'}(\mathbf{r}')u_{\mathbf{k}'c'}(\mathbf{r}') = \\ &= \sum_{ij\alpha}\sum_{mn\beta}\int d\mathbf{r}d\mathbf{r}'\, \langle \mathcal{E}_\alpha|\, E^{\mathbf{k}}_{iv}{E^{\mathbf{k}}_{jc}}^* F^{\alpha *}_{ij}\, |\mathbf{r}\rangle\, \langle \mathbf{r}|\, \hat{v}\, |\mathbf{r}'\rangle\, \langle \mathbf{r}'|\, {E^{\mathbf{k}'}_{mv'}}^* E^{\mathbf{k}'}_{nc'} F^{\beta}_{mn}\, |\mathcal{E}_\beta\rangle = \\ &= \sum_{\alpha\beta} {J^{\mathbf{k}}_{\alpha,vc}}^* J^{\mathbf{k}'}_{\beta,v'c'} v^{\alpha\beta}, \end{aligned} \quad (3.49)$$

where $v^{\alpha\beta} = \langle \mathcal{E}_\alpha|\, \hat{v}\, |\mathcal{E}_\beta\rangle$. The Coulomb potential is written as a sum of Fourier components,

$$v_{\mathbf{q}+\mathbf{G},\mathbf{q}+\mathbf{G}'} = e^{-i(\mathbf{q}+\mathbf{G})\cdot\mathbf{r}}\frac{\delta_{\mathbf{G},\mathbf{G}'}}{|\mathbf{q}+\mathbf{G}||\mathbf{q}+\mathbf{G}'|}e^{i(\mathbf{q}+\mathbf{G}')\cdot\mathbf{r}'}, \quad (3.50)$$

with the term $\mathbf{q} = \mathbf{G} = \mathbf{G}' = 0$ set to zero to take account for local field effects. In addition, we notice that in this case the exponentials included in the wave functions eliminate with each other. This does not occur in the case of the direct kernel term:

$$\begin{aligned} K^{d,\text{bare}}_{\mathbf{k}vc,\mathbf{k}'v'c'} \equiv \langle \mathbf{k}vc|\, K^{d,\text{bare}}\, |\mathbf{k}'v'c'\rangle &= \\ = -\int d\mathbf{r}d\mathbf{r}' u^*_{\mathbf{k}c}(\mathbf{r})u_{\mathbf{k}'c'}(\mathbf{r})e^{i(\mathbf{k}'-\mathbf{k})\cdot\mathbf{r}}v(\mathbf{r},\mathbf{r}')e^{-i(\mathbf{k}'-\mathbf{k})\cdot\mathbf{r}'}u^*_{\mathbf{k}'v'}(\mathbf{r}')u_{\mathbf{k}v}(\mathbf{r}'). \end{aligned} \quad (3.51)$$

Let us note that since we are considering the matrix element with $\mathbf{k}$ and $\mathbf{k}'$ fixed, it is useful to set $\mathbf{k} = \mathbf{q} + \mathbf{G}$ and $\mathbf{k}' = \mathbf{q} + \mathbf{G}'$ and define

$$v_{\mathbf{k}'-\mathbf{k}}(\mathbf{r}, \mathbf{r}') \equiv e^{i(\mathbf{k}-\mathbf{k}')\cdot\mathbf{r}} v(\mathbf{r}, \mathbf{r}') e^{-i(\mathbf{k}-\mathbf{k}')\cdot\mathbf{r}'} = \sum_{\mathbf{G}} \frac{1}{|\mathbf{q}+\mathbf{G}|^2}. \tag{3.52}$$

It is easy to see that when $(\mathbf{q}, \mathbf{G}) = (0, 0)$ such term diverges: it thus must be evaluated in a different way. Our approach was to replace it with a mean of the Coulomb interaction over an appropriate volume $\tilde{\Omega}$ in the first Brillouin zone, namely

$$\frac{1}{|\mathbf{G}|^2} \quad \rightarrow \quad \frac{\Omega}{(2\pi)^3} \int_{\tilde{\Omega}} d\mathbf{q} \frac{1}{|\mathbf{q}+\mathbf{G}|^2}. \tag{3.53}$$

In the case only the $\Gamma$ point ($\mathbf{k} = (0, 0, 0)$) is considered, $\tilde{\Omega}$ is the whole IBZ. On the contrary, one takes the smallest volume defined by k-points grid in which $\Gamma$ is included. The computation of such integral is performed using an appropriate grid, which density is crucial in order to find finite and converged results.
The expression of the direct kernel term with the bare interaction in the optimal bases is then easily obtained:

$$\begin{aligned} K^{d,\text{bare}}_{\mathbf{k}vc,\mathbf{k}'v'c'} &= -\sum_{ij\alpha} \sum_{mn\beta} \int d\mathbf{r} d\mathbf{r}' \langle \mathcal{E}_\alpha | \, E^{\mathbf{k}*}_{ic} E^{\mathbf{k}'}_{jc'}{}^{*} F^{\alpha*}_{ij} \, |\mathbf{r}\rangle \langle \mathbf{r}| \, \hat{v}_{\mathbf{k}'-\mathbf{k}} \, |\mathbf{r}'\rangle \langle \mathbf{r}'| \, E^{\mathbf{k}'}_{mv'}{}^{*} E^{\mathbf{k}}_{nv} F^{\beta}_{mn} \, |\mathcal{E}_\beta\rangle = \\ &= -\sum_{\alpha\beta} J^{\mathbf{k}\mathbf{k}'}_{\alpha,cc'}{}^{*} J^{\mathbf{k}\mathbf{k}'}_{\beta,vv'} v^{\alpha\beta}_{\mathbf{k}'-\mathbf{k}}, \end{aligned} \tag{3.54}$$

where $v^{\alpha\beta}_{\mathbf{k}'-\mathbf{k}} = \langle \mathcal{E}_\alpha | \, \hat{v}_{\mathbf{k}'-\mathbf{k}} \, |\mathcal{E}_\beta\rangle$. The case of the direct interaction term with the screened Coulomb interaction is totally analogous. However, the computation of $W$ is much more demanding than $v$; for that reason we evaluate it at the $\Gamma$ point, then we extrapolate the values for generic $\mathbf{G}$, $\mathbf{G}'$. To show the validity of this approach, we rewrite the definition (1.85) in the form

$$\begin{aligned} W = \varepsilon^{-1} v &= v + v\Pi v + \cdots = v\left[1 + \Pi v + \Pi v \Pi v + \cdots\right] = v \sum_{n=0}^{\infty} (\Pi v)^n \\ &= (1 - \Pi v)^{-1} v. \end{aligned} \tag{3.55}$$

This equation suggests that $\varepsilon^{-1} = (1 - \Pi v)^{-1}$. It is actually convenient to cast the dielectric function in a symmetric form, namely

$$W \equiv v^{\frac{1}{2}} \tilde{\varepsilon}^{-1} v^{\frac{1}{2}} = (1 - v^{\frac{1}{2}} \Pi v^{\frac{1}{2}})^{-1} v. \tag{3.56}$$

Furthermore, it is customary to adopt the diagonal approximation $\tilde{\varepsilon}^{-1}(\mathbf{r}, \mathbf{r}') = \varepsilon_0^{-1} \delta_{\mathbf{r},\mathbf{r}'}$, which yields to the writing

$$\Pi(\mathbf{G}, \mathbf{G}'; \Gamma) = \delta_{\mathbf{G},\mathbf{G}'} (1 - \varepsilon_0) |\mathbf{G}|^2. \tag{3.57}$$

The generalization of such relation for a generic point of the IBZ is simply

$$\Pi(\mathbf{G}, \mathbf{G}'; \mathbf{q}) = \delta_{\mathbf{G},\mathbf{G}'}(1 - \varepsilon_0)|\mathbf{q} + \mathbf{G}|^2, \tag{3.58}$$

and then it is straightforward to attain

$$\Pi(\mathbf{G}, \mathbf{G}'; \mathbf{q}) = \frac{|\mathbf{q} + \mathbf{G}|}{|\mathbf{G}|}\Pi(\mathbf{G}, \mathbf{G}'; \Gamma)\frac{|\mathbf{q} + \mathbf{G}'|}{|\mathbf{G}'|}. \tag{3.59}$$

The last equation is henceforth exploited to extend our knowledge of the screened Coulomb interaction at the $\Gamma$ point to a general point of the IBZ. In conclusion, this approximated method allows to avoid the computationally expensive procedure of the estimation of the $W$ at many k-points.

### 3.4.3 Research of a minimum: steepest descent and conjugate gradient

The knowledge of the kernel interaction term allows us to apply the quasi-particle Hamiltonian to a generic state $S$ , defined by the expansion coefficients $A^S_{vc}$. However, an additional algorithm for the search of the state with minimum energy $\Omega_S$ is needed. Our approach is to adopt iterative methods that find the state $|x\rangle$ which minimizes the energy function $E(x) = \langle x| H |x\rangle$, using a random normalized state $|x_0\rangle$ as a starting point.
The simplest method implemented in this work is known as *steepest descent*, and consists in the use of the update formula

$$|x_{i+1}\rangle = |x_i\rangle - H |x_i\rangle ; \tag{3.60}$$

let us note that $H |x_i\rangle$ is nothing but the gradient of the function $E(x)$. In other terms, the steepest descent algorithm looks for the minimum in the opposite direction with respect to the one given by the gradient of the energy.
Although converged results are in this way attained, it is convenient to adopt the *conjugate gradient* method, which yields to the same results in a number of steps 5-10 times lower than steepest descent. After a first steepest descent step, the energy function is approximated to a parabola. Taken then the vectors $|x_i\rangle$, $|x_i + \alpha h_i\rangle$ and $|x_i + 2\alpha h_i\rangle$ with $|h_i\rangle$ search direction (initially set to $H |x_i\rangle$) and $\alpha$ user defined parameter, $|x_{i+1}\rangle$ is defined as the vector corresponding to the minimum of the parabola selected by such vectors. Consequently, the research direction is updated via the equation

$$|h_{i+1}\rangle = \gamma |h_i\rangle + H |x_i\rangle \qquad \text{with} \qquad \gamma = \frac{|H |x_{i+1}\rangle |^2}{|H |x_i\rangle |^2}. \tag{3.61}$$

This is not the whole scheme described in [24]: the normalization of the states did not allow the implementation of the improvement of the gradient.
In addition, the improving of the search direction step by step however tends to be less

efficient with the increasing of the number of iterations. To obviate to such issue one can simply restart the method every a fixed amount of steps (20 in our case) with a steepest descent step.
In order for the second, third, etc. minimum excitonic energy to be found, the procedure is exactly the same a part from the fact we have to limit our research on the Hilbert space not spanned by the eigenvectors relative to the already found eigenstates.

**Algorithm 4** Conjugate gradient

randomize $|x\rangle$
$|h\rangle = H\,|x\rangle$
**repeat**
  find parabola passing through $|x\rangle$, $|x\rangle + \alpha\,|h\rangle$, $|x\rangle + \alpha\,|h\rangle$
  $|x\rangle \to$ parabola lowest point
  $\gamma = \dfrac{|H\,|x_{i+1}\rangle\,|^2}{|H\,|x_i\rangle\,|^2}$
  $|h\rangle \to \gamma\,|h\rangle + H\,|x\rangle$
**until** convergence is reached

# Chapter 4

# Convergence tests

This chapter is dedicated to the presentation of several tests on the convergence of the methods adopted.
At first results of calculations on simple molecules are presented, using CO and $CH_3NH_3$ as benchmarks; both relaxation and electronic structure calculations were performed in order to estimate the ideal plane wave energy cutoff discussed in §3.1.
An example of calculation of infrared dielectric constant is then exhibited, as a complement to our investigation on dielectric properties of complex systems.
Afterward the code for the BSE solving is tested: starting from a study on the performance of the methods for the excitonic energies evaluation, such results are discussed at different values of the cutoff parameters adopted in the optimal bases construction. The energies attained are then confronted with those estimated by the `Yambo` code ([23]) for a system composed by 8 atoms of silicium with a $2 \times 2 \times 2$ $k$-points grid.
The convergence of the optical spectrum is finally studied with the variation of the number of $k$ points considered along with the number of Lanczos steps performed during the application of the Haydoch recursive method.

## 4.1 DFT computations

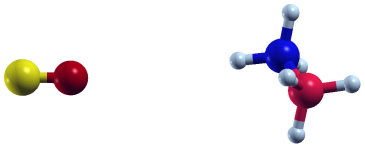

(a) (b)

Figure 4.1: $CH_3NH_3$ and CO molecules.

The code adopted for DFT computations is contained in the `pw` package within `QE`. Provided the atom types and positions along with suitable pseudopotentials, relaxation,

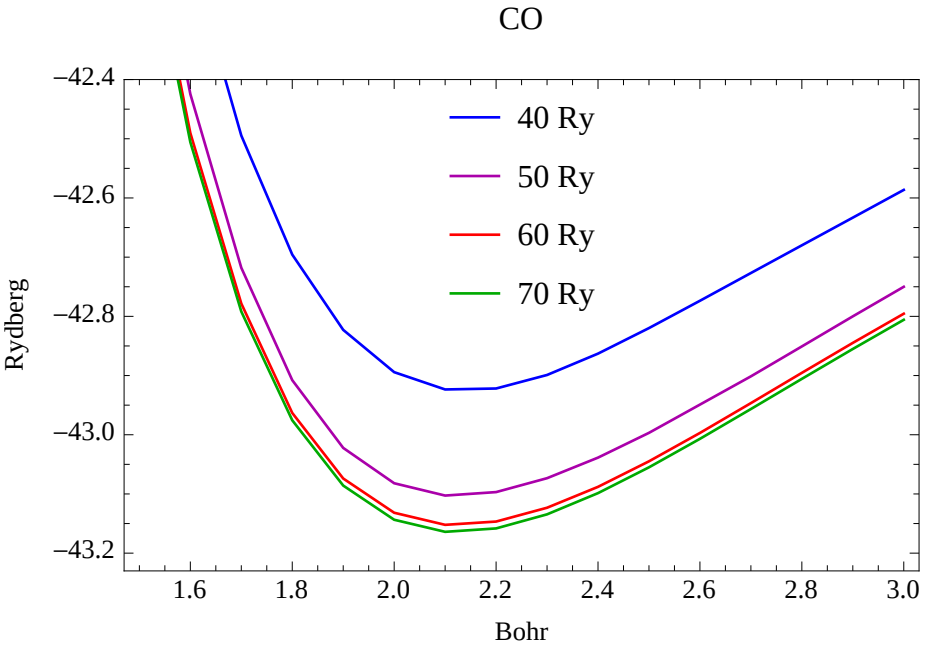


Figure 4.2: Results of self-consistent calculations on CO with cutoff energy $E^* = 40, 50, 60, 70\ Ry$. The $x$ axis corresponds to the interatomic distance, while the $y$ axis is the total energy of the molecule.

self-consistent and not-self-consistent band structure calculations can be performed. As explained in §3.1, only the plane waves within a certain user defined cutoff energy $E^*$ are considered. Since the verification of the reaching of convergence is of fundamental importance, some reliable physical quantity must be observed under variation of $E^*$. Not all physical quantities are indeed suitable for this objective. Take as an example the total energy of a molecule: for the fact it changes with parameters such as the dimension of the Bravais cell or the pseudo potential adopted, its confrontation with other calculations or experimental data can be misleading. Moreover, one is usually interested more in the bound energy of the molecule than in the total energy of the system. It is thus convenient to consider quantities like interatomic distances, which must be in any case the same for the same molecule.

As an example, we present some results of self-consistent calculations in the LDA approximation for the monoxide molecule. The distance between the two atoms is set at different values for several cutoff energies ($E^* = 40, 50, 60, 70\ Ry$), and for each case the total energy is evaluated. It is easy to see from fig. 4.2 that the highest $E^*$ is, the closest at convergence the energy seems to be. However, from table 4.1 we see that the intermolecular distance reaches a good level of convergence before the binding energy does ($E^* = 50\ Ry$). Once $d_{min}$ is estimated, the vibrational energy of the molecule can be readily evaluated; it is then interesting to note that all the results with $E^*$ higher than 40 $Ry$ are compatible with the experimental value $E_{vibe}^{exp} = 0.1298\ eV$ within the fit error.

We then conclude that a good cutoff energy for our DFT calculations can be set at $E^* = 50\ Ry$.

| $E^*$ [Ry] | $E_{min}$ [Ry] | $d_{min}$ [Bohr] | $E_{vib}$ [eV] |
|---|---|---|---|
| 20 | -41.088 | 2.46371 | 0.0864 ± 0.0088 |
| 40 | -42.926 | 2.15486 | 0.1410 ± 0.0405 |
| 50 | -43.106 | 2.14252 | 0.1451 ± 0.0440 |
| 60 | -43.155 | 2.14225 | 0.1433 ± 0.0423 |
| 70 | -43.167 | 2.14140 | 0.1436 ± 0.0420 |

Table 4.1: Binding energy $E_{min}$, intermolecular distance $d_{min}$ and relative vibrational energy of the carbon monoxide molecule at different cutoff values $E^*$.

### 4.1.1 Infrared spectrum of methylammonium

The infrared contribution to the dielectric function can be as well evaluated via a combination of self-consistent calculations using the `pw` package.
The dynamical matrix (2.4) can be cast in the form

$$D^{i,j}_{\mu\nu} = -\frac{1}{\sqrt{m_i m_j}} \left( \frac{\partial F^i_\mu}{\partial u^j_\nu} \right) \Bigg|_{u^\mu_i = 0 = u^\nu_j} \cong -\frac{1}{\sqrt{m_i m_j}} \frac{F^i_\mu(\mathbf{R} + h\mathbf{e}^j_\nu) - F^i_\mu(\mathbf{R} - h\mathbf{e}^j_\nu)}{2h} \tag{4.1}$$

approximating the first derivative with a finite difference. The notation $F^i_\mu(\mathbf{R} \pm h\mathbf{e}^j_\nu)$ stands for the $\mu$ direction of the force acting on the $i$-th atom when the atom $j$ is moved from the equilibrium position $\mathbf{R}$ of a quantity $\pm h$ in the direction $\nu$, with $i, j = 1, \ldots, N$ and $\mu, \nu = 1, 2, 3$. The computation of the dielectric matrix then require $N \times 3 \times 2$ self consistent calculations, one for a forward and one for a backwards displacement of each atom in each direction.
In a similar way the expression

$$Z^{\alpha\,*}_{i\mu} = \left( \frac{\partial F^i_\mu}{\partial \mathcal{E}_\alpha} \right) \Bigg|_{u^\mu_i = 0 = \mathcal{E}_\alpha} \cong \frac{\left(F^i_\mu\right)\big|_{\mathcal{E}_\alpha = h} - \left(F^i_\mu\right)\big|_{\mathcal{E}_\alpha = -h}}{2h} \tag{4.2}$$

is attained for the Born effective charge. Here $(F^i_\mu)|_{\mathcal{E}_\alpha = h}$ denotes the $\mu$ direction of the total force acting on the $i$th atom when an electric field of intensity $\pm h$ is applied in the direction $\alpha$.
Such calculations were executed for the methylammonium ($CH_3NH_3$). Since LSDA does not succeed in the representation of molecular spin states, the HOMO (Highest Occupied Molecular Orbital) is found to be degenerate. This fact implies a not well defined band structure around the Fermi level. As a consequence, it can be treated as a metallic system, in which the absence of a gap leads to the overlapping of conduction and valence states. To cope with this issue the charge density around the Fermi level is

replaced with a certain distribution function, common choices of which are Fermi-Dirac and gaussian distributions. The use of such method introduces an artificial temperature $T$ and limit for its vanishing must be taken for ground state results to be recovered. In order to simplify the estimation of such limit also non physical distribution can be used. The approach above described is known as *smearing*.

| Vibrational frequencies $[cm^{-1}]$ | | | |
|---|---|---|---|
| 3104.26 | 1380.79 | 1193.16 | 852.51 |
| 3098.43 | 1380.41 | 1189.96 | 278.337 |
| 3002.28 | 1332.77 | 964.162 | 68.9172 |
| 2910.42 | 1279.15 | 855.014 | 33.7191 |

Table 4.2: Vibrational frequencies for methylammonium molecule ($CH_3NH_3$)

## 4.2 Convergence and efficiency tests on silicium cluster

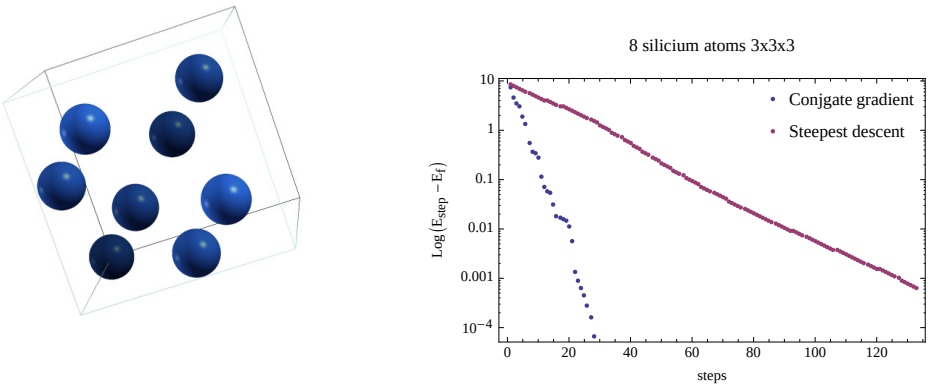


(a) (b)

Figure 4.3: Primitive cell of 8 silicium atoms in cluster structure (left) and convergence tests of steepest descent (red) and conjugate gradient (blu) algorithms for the lowest excited state for bulk silicium with a $3 \times 3 \times 3$ k-point grid (right).

The purpose of this section is to conduct a study on the efficiency and convergence properties of both the BSE solving approach and the method employed for the computation of the optical spectrum. As first, the variation of the lowest excitation energy computed with BSE is analyzed under variation of the threshold parameters $s_{pw}$ and $s_{prod}$ defined in §3.4. Then the consequence of the same thresholds on the spectrum is

analyzed, along with the convergence with the number of Lanczos steps and of k-points considered.

The system here adopted is composed by 8 silicium atoms in a bulk structure, which is of fundamental importance in the field of microelectronics. Since our approach is ideated for systems of remarkable size, we expect it to be not so efficient for the silicon for its reduced dimensions. For the same reason, convergence could be more difficult to be reached with respect to the case of larger structures.
The minimization method used in the calculations will be always the conjugate gradient, for the fact its efficiency is, as announced, much better than the steepest descent's one. Such feature is evident from fig. 4.3 (b), where the logarithm of the difference between the lowest energy estimated at a certain step and the converged value is displayed for each step and both methods. The difference between the two cases is striking: steepest descent needs about 7 times the steps the conjugate gradient does for convergence to be reached. It is also possible to observe that the latter slows down in the whereabouts of step 20, and then speeds up again: that is nothing but the effect of the restarting of the algorithm.
However, the conjugate gradient algorithm as implemented sometimes happens to be unstable: the energy estimated at a certain step is not always lower than the one relative to the previous step. In such cases the procedure effects a steepest descent step. This may cause an increment of computation times.
For each computation the method is performed until a certain precision is attained, typically $10^{-4}\ eV$. Nevertheless the several approximations adopted imply the reliability of the results only within $0.01\ eV$.

### 4.2.1 Optimal basis thresholds and excitonic energies

The system here is considered with different values of k-point grids, $2 \times 2 \times 2$ and $3 \times 3 \times 3$. In each case the lowest excitonic energies were computed for the TDH, TDHF and BSE approximations. Results of their calculation with different values of the thresholds $s_{pw}$ and $s_{prod}$ are shown in the tables below, along with the numbers $n_e$, $n_{\mathcal{E}}$ of vectors of the optimal bases and the time $t_{basis}$ necessary for the computation of both the optimal bases and the coefficients linking the old bases with the new ones.
Since the total number of states is set to 32 (16 conduction, 16 valence), the dimension of the original basis for the periodic part of the wave functions $u_{\mathbf{k}\lambda}$ is $32 \times 2^3 = 256$ and $32 \times 3^3 = 864$ for the different grids. The plane waves threshold is set at different values ranging from $10^{-2}$ to 1, and (tables 4.3 and 4.4). We note that choosing higher $s_{pw}$s is senseless for the fact 32 is exactly the number of $u_{\mathbf{k}\lambda}$s for one k-point, namely the starting vectors for the construction of the optimal basis. It is evident that the variation of $s_{pw}$ does not affect at all TDH and BSE energies, while TDHF ones undergo some few tens of $meV$ modifications. On the other hand, the dimension of the first optimal basis, $n_e$, is significantly reduced, along with the computation times.
Comparing the number of vectors selected with the different grids we see that they are quite similar. On the contrary, the higher number of k-points is considered the greater the computation times are modified under variation of $s_{pw}$, and the more the procedure

| $s_{pw}$ | $s_{prod}$ | $n_e$ | $n_{\mathcal{E}}$ | $t_{basis}$ $[s]$ | $E_{TDH}$ $[eV]$ | $E_{TDHF}$ $[eV]$ | $E_{BSE}$ $[eV]$ |
|---|---|---|---|---|---|---|---|
| $1 \cdot 10^{-2}$ | $10^{-1}$ | 96 | 887 | 413 | 1.305087 | -2.107939 | 1.079958 |
| $2 \cdot 10^{-2}$ | $10^{-1}$ | 78 | 761 | 256 | 1.305971 | -2.106089 | 1.081464 |
| $5 \cdot 10^{-2}$ | $10^{-1}$ | 64 | 577 | 184 | 1.305131 | -2.095527 | 1.082766 |
| $1 \cdot 10^{-1}$ | $10^{-1}$ | 59 | 454 | 164 | 1.305168 | -2.090025 | 1.083149 |
| $3 \cdot 10^{-1}$ | $10^{-1}$ | 51 | 398 | 154 | 1.305640 | -2.076817 | 1.080428 |
| $5 \cdot 10^{-1}$ | $10^{-1}$ | 39 | 343 | 144 | 1.306350 | -2.064159 | 1.083345 |
| $1 \cdot 10^{0}$ | $10^{-1}$ | 32 | 223 | 139 | 1.306794 | -2.059091 | 1.080803 |

Table 4.3: Results of calculations on 8 silicium atoms in bulk structure with $2 \times 2 \times 2$ k-points grid with threshold for periodic parts of the wave functions optimal basis construction set to $10^{-1}$.

| $s_{pw}$ | $s_{prod}$ | $n_e$ | $n_{\mathcal{E}}$ | $t_{basis}$ $[s]$ | $E_{TDH}$ $[eV]$ | $E_{TDHF}$ $[eV]$ | $E_{BSE}$ $[eV]$ |
|---|---|---|---|---|---|---|---|
| $1 \cdot 10^{-2}$ | $10^{-1}$ | 100 | 919 | 2639 | 1.252138 | -0.978499 | 1.167665 |
| $2 \cdot 10^{-2}$ | $10^{-1}$ | 88 | 788 | 1574 | 1.252138 | -0.976382 | 1.167738 |
| $5 \cdot 10^{-2}$ | $10^{-1}$ | 79 | 601 | 839 | 1.252144 | -0.968817 | 1.167927 |
| $1 \cdot 10^{-1}$ | $10^{-1}$ | 73 | 550 | 632 | 1.252151 | -0.969400 | 1.167902 |
| $3 \cdot 10^{-1}$ | $10^{-1}$ | 59 | 424 | 354 | 1.252194 | -0.960838 | 1.168083 |
| $5 \cdot 10^{-1}$ | $10^{-1}$ | 53 | 383 | 323 | 1.252239 | -0.956650 | 1.168286 |
| $1 \cdot 10^{0}$ | $10^{-1}$ | 32 | 220 | 166 | 1.252403 | -0.955805 | 1.168176 |

Table 4.4: Results of calculations on 8 silicium atoms in bulk structure with $3 \times 3 \times 3$ k-points grid with threshold for periodic parts of the wave functions optimal basis construction set to $10^{-1}$.

is effective. The time necessary for bases and matrices construction, $t_{basis}$, for $s_{pw} = 1$ is reduced by a factor 3 with respect to the case $s_{pw} = 0.01$ for the 8 k-points grid, compared to a factor 16 for the 27 k-points grid.
As a conclusion, we can affirm that for this system the choice $s_{pw} = 0.1$ guarantees an good level of convergence for the lowest excitonic energy under each degree of approximation.

In tables 4.5 and 4.6 $s_{pw}$ is fixed to 1, while the product basis threshold varies instead. The lowest excitation energy is not notably altered for values of the products threshold below $10^{-1}$, then it tends to gradually deteriorate (especially in the TDHF approximation). Here the computation times do not change significantly, but the number of elements of the product basis $n_{\mathcal{E}}$ undergoes important modifications. Let us recall that for such value of the $u_{\mathbf{k}\lambda}$ optimal basis, in the absence of a second cutoff, the number of products is $32^2 = 1024$. It is then evident that less than one fourth of such vectors ($s_{prod} = 0.1$) actually contributes to the final estimate of the excitation energies.

Finally, confrontation with results obtained for the same system ($2 \times 2 \times 2$ k-points grid) by the `yambo` code [23] is displayed. The agreement between the two computa-

| $s_{pw}$ | $s_{prod}$ | $n_e$ | $n_{\mathcal{E}}$ | $t_{basis}$ $[s]$ | $E_{TDH}$ $[eV]$ | $E_{TDHF}$ $[eV]$ | $E_{BSE}$ $[eV]$ |
|---|---|---|---|---|---|---|---|
| 1 | $10^{-7}$ | 32 | 618 | 151 | 1.307242 | -2.070908 | 1.085004 |
| 1 | $10^{-3}$ | 32 | 497 | 152 | 1.307231 | -2.070927 | 1.084997 |
| 1 | $10^{-2}$ | 32 | 341 | 145 | 1.307198 | -2.070669 | 1.084994 |
| 1 | $10^{-1}$ | 32 | 223 | 139 | 1.306794 | -2.059473 | 1.080803 |
| 1 | $5 \cdot 10^{-1}$ | 32 | 146 | 163 | 1.303317 | -2.057536 | 1.071689 |
| 1 | 1 | 32 | 60 | 137 | 1.293850 | -2.107269 | 1.051160 |
| 1 | 2 | 32 | 15 | 143 | 1.284351 | -2.308060 | 1.070924 |
| 1 | 3 | 32 | 3 | 142 | 1.276295 | -0.725708 | 1.168078 |

Table 4.5: Results of calculations on 8 silicium atoms in bulk structure with $2 \times 2 \times 2$ k-points grid with threshold for products optimal basis construction set to 1.

| $s_{pw}$ | $s_{prod}$ | $n_e$ | $n_{\mathcal{E}}$ | $t_{basis}$ $[s]$ | $E_{TDH}$ $[eV]$ | $E_{TDHF}$ $[eV]$ | $E_{BSE}$ $[eV]$ |
|---|---|---|---|---|---|---|---|
| 1 | $10^{-7}$ | 32 | 618 | 268 | 1.252557 | -0.962757 | 1.168041 |
| 1 | $10^{-3}$ | 32 | 494 | 229 | 1.252554 | -0.962764 | 1.168038 |
| 1 | $10^{-2}$ | 32 | 343 | 192 | 1.252553 | -0.962756 | 1.168037 |
| 1 | $10^{-1}$ | 32 | 220 | 166 | 1.252403 | -0.955901 | 1.168175 |
| 1 | $5 \cdot 10^{-1}$ | 32 | 123 | 163 | 1.251274 | -0.951897 | 1.167194 |
| 1 | 1 | 32 | 61 | 153 | 1.249440 | -1.190540 | 1.167065 |
| 1 | 2 | 32 | 16 | 149 | 1.245436 | 0.039351 | 1.184393 |
| 1 | 3 | 32 | 3 | 151 | 1.243747 | 0.080141 | 1.198208 |

Table 4.6: Results of calculations on 8 silicium atoms in bulk structure with $3 \times 3 \times 3$ k-points grid with threshold for products optimal basis construction set to 1.

tions is quite good, in particular for the TDH approximation. The origin of the (slight) difference in the other two approximations probably lies in the different way of the treatment of the Coulomb divergence. In addition, for the BSE case, the difference in the approaches adopted for the calculation of the screened interaction, including the extrapolation of $W$ at any $\mathbf{k}$ from $\Gamma$, could play an important role.

We then conclude that the choice $s_{pw} = 0.1 = s_{prod}$ for the optimal bases thresholds leads to reliable and converged results.

| | Yambo | $s_{pw}, s_{prod} = 0.1$ |
|---|---|---|
| TDH $[eV]$ | 1.29 | 1.31 |
| TDHF $[eV]$ | $-2.16$ | $-2.09$ |
| BSE $[eV]$ | 1.17 | 1.08 |

Table 4.7: Confrontation with `yambo` code.

### 4.2.2 Convergence of optical spectra

Once a good set of threshold parameters for the evaluation of the excitonic (BSE) Hamiltonian has been determined, it is important to study the consequences of the optimal bases on the optical spectrum. The function considered for such examination is the mean of the imaginary part of the dielectric function over the directions $\hat{q} = \hat{x}, \hat{y}, \hat{z}$, namely

$$\varepsilon_2 = \frac{1}{3}\left(\varepsilon_2^{\hat{x}} + \varepsilon_2^{\hat{y}} + \varepsilon_2^{\hat{z}}\right). \tag{4.3}$$

For each direction the Haydoch recursive method is applied with the same number of Lanczos steps and values of $s_{pw}$, $s_{prod}$ and of the infinitesimal $\eta$.
We once again adopt the $2 \times 2$ k-points grid to perform our tests. From fig. 4.4 we evince that the value 0.1 for both the thresholds is a good choice also in this case (as we expected). Such results were obtained with 100 Lanczos steps (per direction). Fig. 4.5 shows that the more Lanczos iterations are considered the more the spectrum gains details. Nevertheless, very little difference occurs between the cases of 50 and 75 iterations.
The number of k-points remarkably affects the outcome of the calculation (see fig. 4.6). The denser the grid is considered, the more information can be correctly extrapolated with the Shirley approach. It is evident that the $2 \times 2 \times 2$ grid is not nearly enough to obtain converged spectra; it is anyway useful to be considered for a study of the influence of the other parameters for its reduced computational time. On the other hand, the$5 \times 5 \times 5$ k-point grid yields to results close to convergence since they are comparable to the ones displayed in fig. 8 of [17] (Rohlfing, Louie), as shown in 4.7b. The value of $\eta$ is set to 0.013 $Ry = 0.18\ eV$ to match the data of that paper. This parameter is not a physical but an arbitrary quantity, and controls the broadening of the spectrum (fig. 4.7a). It is then important to select an appropriate value in order to attain a spectrum comparable to experiments. Rolfing and Louie set the (presumably gaussian) broadening to 0.015 $eV$; this different choice might be a cause of the difference in the two results.
Another notable aspect is that our estimate of the dielectric function is shifted by few tens of eV with respect to the others. That is most likely due to the fact that the $LDA$ energies which are the starting point of the calculation (see 3.46) underestimates the band gap. As a consequence, the dielectric function must be shifted by the value of the quasi-particle band gap correction. It is then possible that our $GW$ calculation dow not estimate such correction as correctly as Rohlfing and Louie's does.

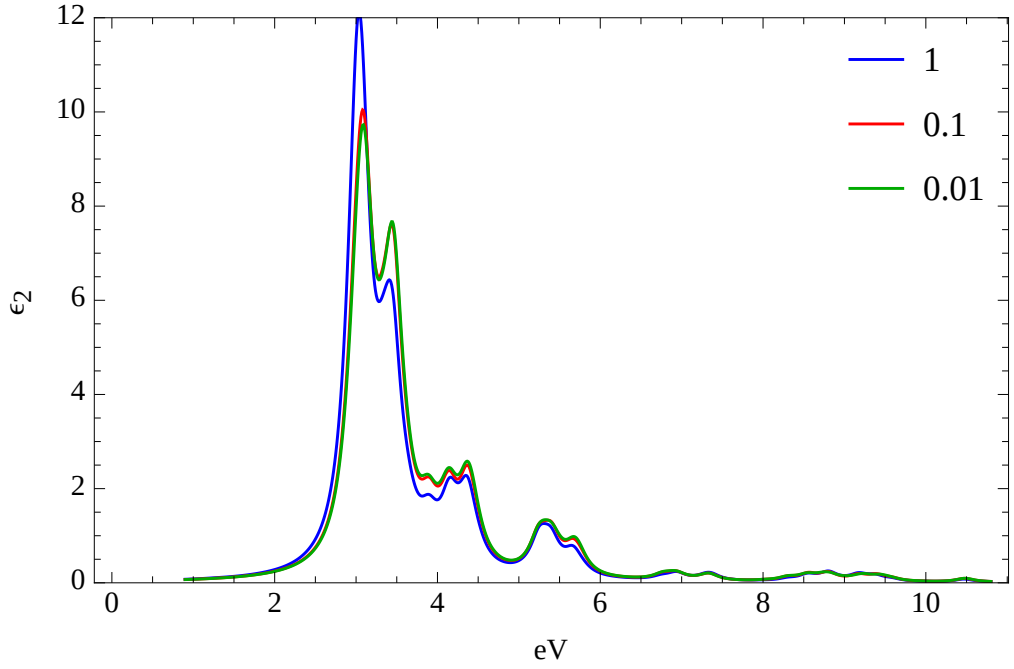


(a) Imaginary part of the dielectric function for $s_{pw} = 1, 0.1, 0.01$.

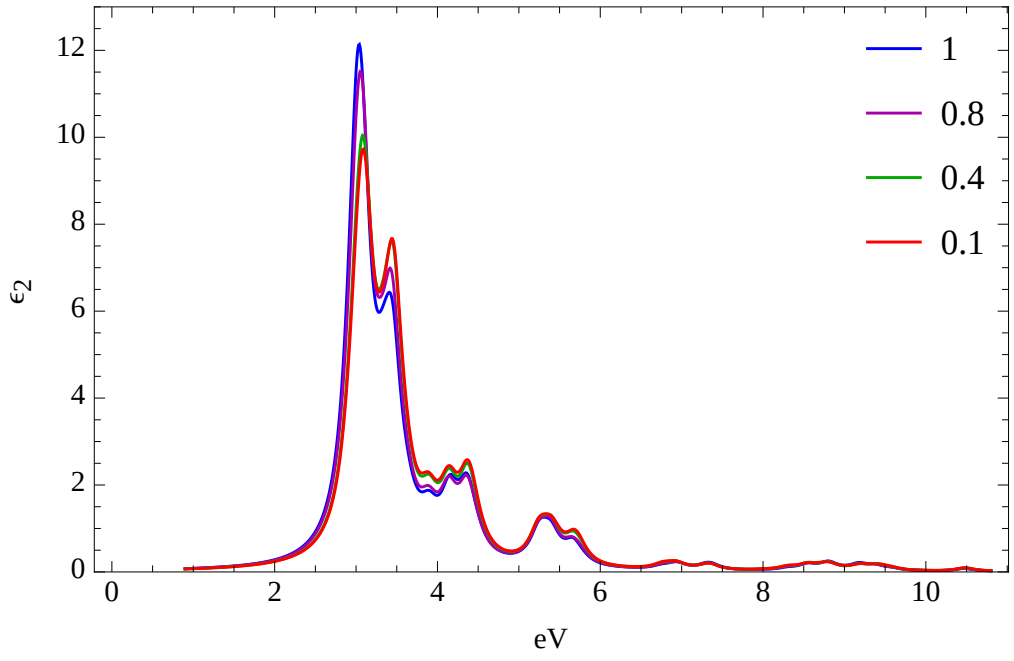


(b) Imaginary part of the dielectric function for $s_{prod} = 1, 0.1, 0.001$.

Figure 4.4: Imaginary part of the dielectric function for 8 silicium atoms in bulk structure with $2 \times 2 \times 2$ k-points grid, $\eta = 0.01$ $Ry$ and 100 Lanczos steps calculated with different values of the optimal bases thresholds.

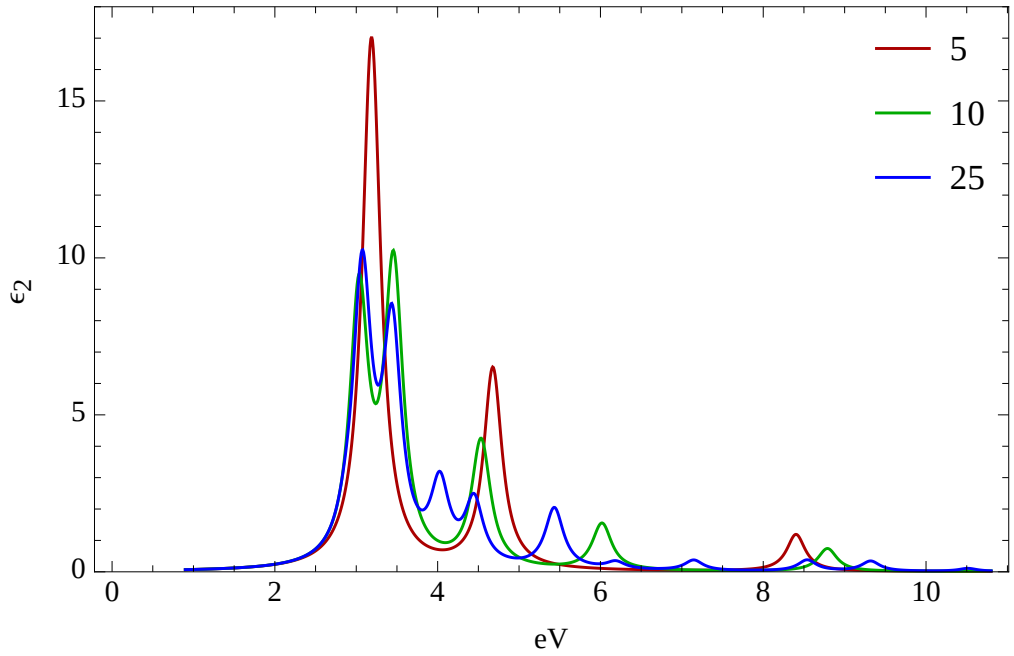


(a) Imaginary part of the dielectric function for 5, 10 and 25 Lanczos steps.

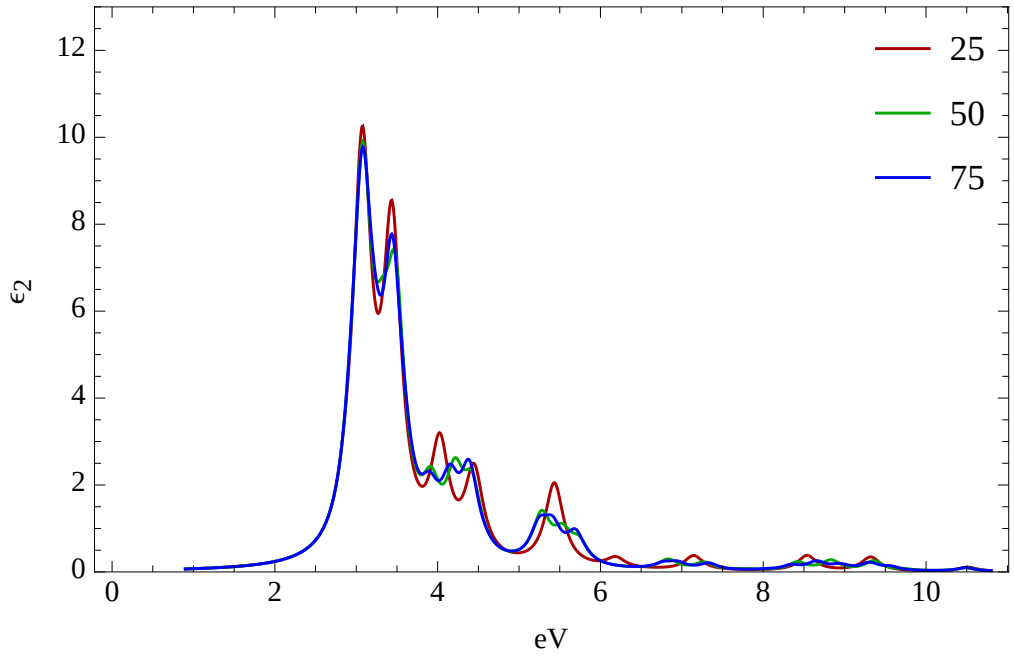


(b) Imaginary part of the dielectric function for 25, 50 and 75 Lanczos steps.

Figure 4.5: Imaginary part of the dielectric function for 8 silicium atoms in bulk structure with $2 \times 2 \times 2$ k-points grid, $s_{pw} = 0.1$, $s_{prod} = 0.1$, $\eta = 0.01$ $Ry$ calculated with different number of Lanczos steps.

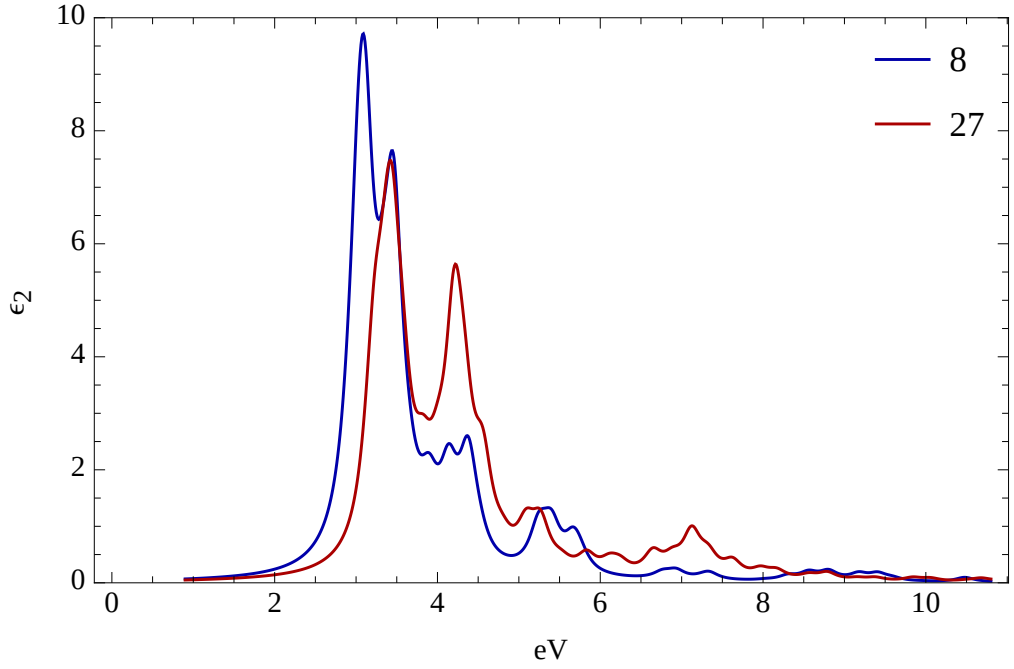


(a) Imaginary part of the dielectric function with $2 \times 2 \times 2$ and $3 \times 3 \times 3$ k-points grids.

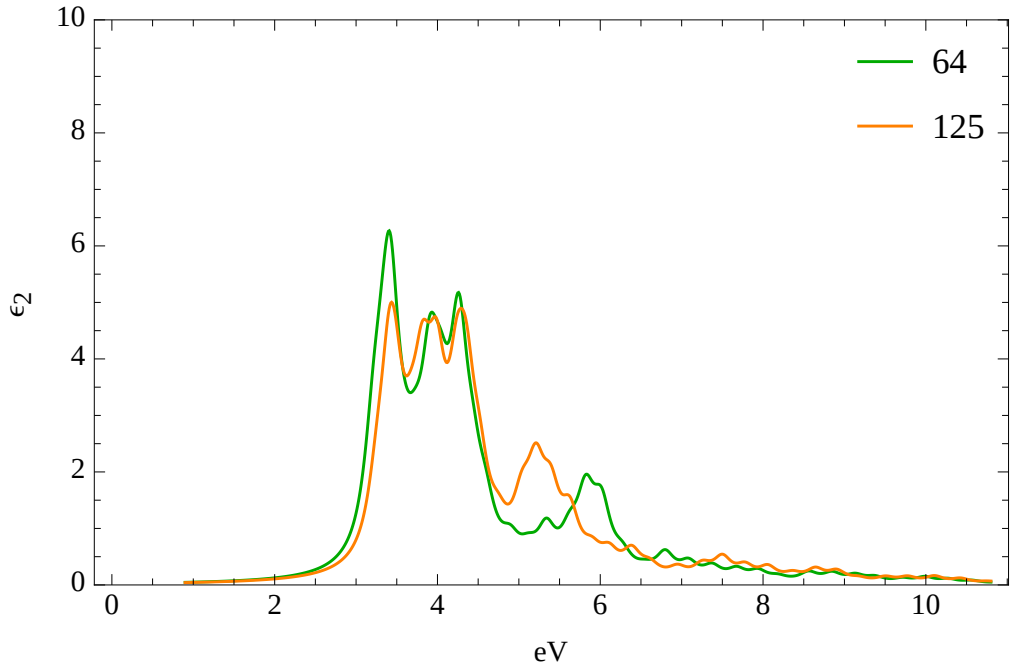


(b) Imaginary part of the dielectric function with $4 \times 4 \times 4$ and $5 \times 5 \times 5$ k-points grids.

Figure 4.6: Imaginary part of the dielectric function for 8 silicium atoms in bulk structure with 100 Lanczos steps, $s_{pw} = 0.1$, $s_{prod} = 0.1$, $\eta = 0.01$ $Ry$ calculated with different k-points grids.

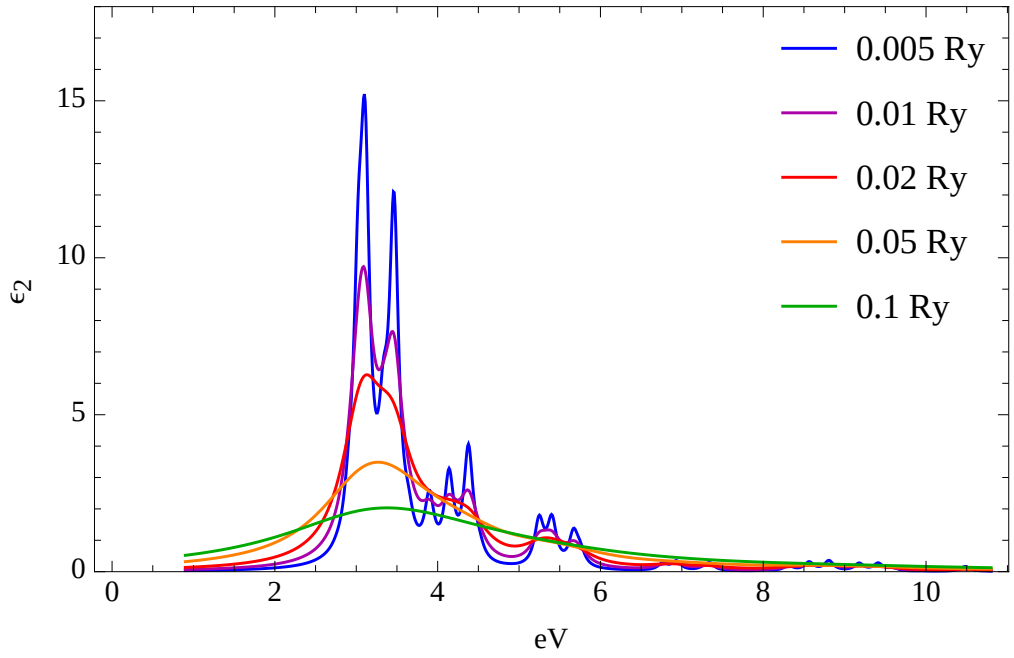


(a) Imaginary part of the dielectric function for 8 silicium atoms in bulk structure with $2 \times 2 \times 2$ k-points grid, $s_{pw} = 0.1$, $s_{prod} = 0.1$, 100 Lanczos steps calculated with different values of $\eta$.

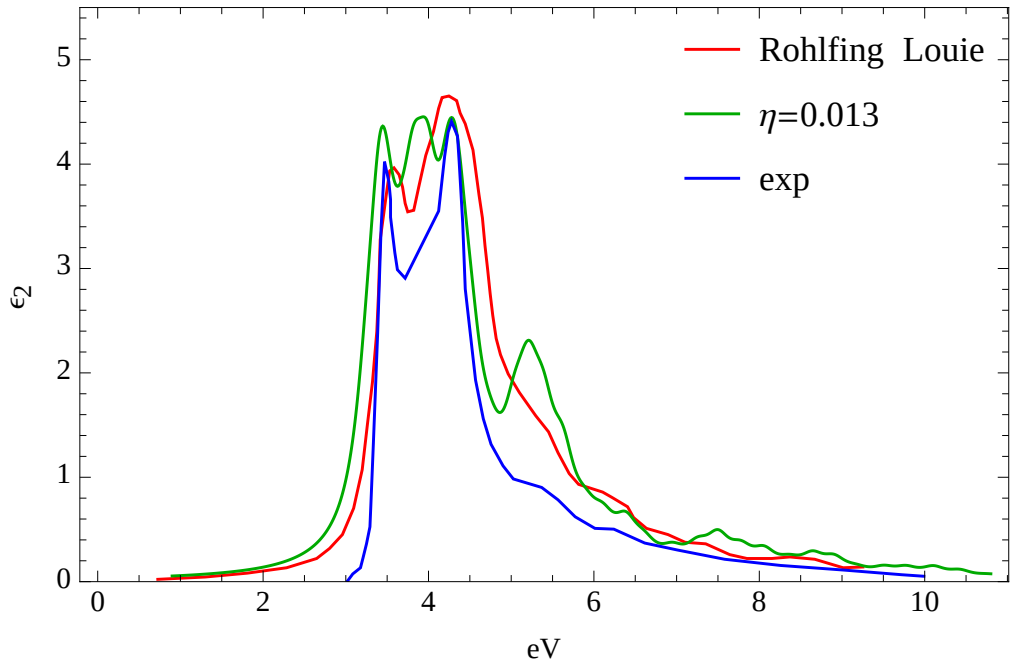


(b) Imaginary part of the dielectric function for 8 silicium atoms in bulk structure computed with 100 Lanczos steps, $s_{pw} = 0.1$, $s_{prod} = 0.1$, $\eta = 0.011$ $Ry$ and $5 \times 5 \times 5$ k-points grid. Such result is compared to the experimental and theoretical ones obtained by Rohlfing and Louie.

Figure 4.7

# Chapter 5

# Conclusions

We considered a many-atom system and described an efficient approach for the computation of its optical spectrum comprehensive of electron-hole interactions.

After an overview of DFT methods Green's function theory was exploited in order to achieve Hedin's equations. A solution of such system is then proposed within the GW approximation, and hence a correction to DFT single-particle energies along with an expression for the screened Coulomb interaction is attained. Consequently, the Bethe-Salpeter is recovered and transformed into an eigenvalue equation which solution yields the excitons eigenstates and eigenvalues. An efficient procedure for the treating of such eigenproblem involving the construction of optimal bases is then displayed.
The performance of the approach is tested using a system composed by 8 cilium atoms as benchmark. The optimal bases were proven to effectively reduce the bases dimensions and, as a consequence, computational costs, without any loose of accuracy. Usable values of the thresholds are indicated and the results found are in good agreement with the ones obtained with the Yambo code.

The knowledge acquired with the solving of the BSE is finally employed in the evaluation of the imaginary part of the dielectric function. The Haydoch recursive method produces converged results with a reduced (100) number of Lanczos steps. The convergence of the spectrum with the number of k-points is then discussed, along with the differences between our results and the ones displayed by Rohlfing and Louie in [17].

# Bibliography


[1] L. C. Allen, A. M. Karo, *Basis Functions for Ab Initio Calculations*, Revs. Mod. Phys. 32 (2): 275–, (1960).

[2] P. Hohenberg and W. Kohn, *Inhomogeneous electron gas*, Phys. Rev. 136, B864 (1964).

[3] W. Kohn and L. J. Sham, *Self-Consistent Equations Including Exchange and Correlation Effects*, Phys. Rev. 140, 4A (1965).

[4] M. van Schilfgaarde, T. Kotani and S. Faleev , *Quasiparticle Self-consistent GW theory*, Phys. Rev. Lett. 96, 226 402 (2006).

[5] A. L. Fetter, J. D. Walecka, *Quantum theory of many-particle systems*, Dover publications, Inc., Mineola (New York), (2002).

[6] G. Strinati, *Application of the Green's functions method to the study of the optical properties of semiconductors*, Riv. Nuovo Cimento 11, 1-86, (1988).

[7] R. M. Martin, *Electronic Structure: Basic Theory and Practical Methods*, Cambridge University Press, (2008).

[8] M. Levy, J. P. Perdew, V. Sahni, *Exact differential equation for the density and ionization energy of a many-particle system*, Phys. Rev. A 30:2745, (1984).

[9] W. M. C. Foulkes, L. Mitas, R. J. Needs, and G. Rajagopal, *Quantum Monte Carlo simulations of solids*, Rev. Mod. Phys. 73, 33 (2001).

[10] Kunc K. and Martin R. M. , in *Ab initio calculation of phonon spectra*, Eds. J. T. Devreese, V. E. van Doren and P. E. van Camp (Plenum, New York), pp 65-99 (1983).

[11] P. Y. Yu, M. Cardona, *Fundamentals of Semiconductors- Physics and Materials Properties*, Springer, (1996).

[12] R. J. Elliott, *Intensity of Optical Adsorption by Excitons*, Phys. Rev. 108, 6 (1957).

[13] L. Hedin, *New method for calculating the one-particle Green's function with application to the electron-gas problem*, Phys. Rev. 139(1965).

[14] L. Hedin and S. Lundqvist, Solid State Phys. 23, 1 (1969).

[15] M. S. Hybertsen and S. G. Louie, *Electron correlation in semiconductors and insulators: Band gaps and quasiparticle energies*, Phys. Rev. B 34, 5390 (1986).

[16] S. Albrecht, L. Reining, R. Del Sole, G. Onida, *Excitonic effects in the optical properties*, phys. stat. sol. 179, 189 (1998).

[17] M. Rohlfing, S. G. Louie, *Electron-hole excitations and optical spectra from first principles*, Phys. Rev. B 62, 8 (2000).

[18] Z. H. Levine, D. C. Allan, Phys. Rev. Lett. 63,16 (1989).

[19] P. Giannozzi et al., J. Phys. Condens. Matter 21, 395502 (2009).

[20] G. Grosso, G. Pastori Paravicini, *Solid State Physics-Second Edition*, Academic Press, 2014.

[21] P. Umari, G. Stenuit, S. Baroni, Phys. Rev. B 79 (2009) 201104(R).

[22] P. Umari, G. Stenuit, S. Baroni, Phys. Rev. B 81 (2010) 115104.

[23] A. Marini, C. Hogan, M. Grüning, D. Varsano, *Yambo: an ab initio tool for excited state calculations*, Comp. Phys. Comm. 180, 1392 (2009).

[24] W. H. Press, S. A. Teukolsky, W. T. Vetterling, B. P. Flannery, *Numerical recipes*, Cambridge University Press (2007).

[25] E. Anderson et al., *LAPACK Users' Guide - Third edition*, Society for Industrial and Apllied Mathematics (1999).

[26] C. L. Lawson et al., *Basic Linear Algebra Subprograms for FORTRAN usage*, ACM Trans. Math. Software 5 (1979).

[27] N. Marzari, D. Vanderbuilt, *Maximally localized generalized Wannier functions for composite energy bands*, Phys. Rev. B 56, 12847 (1997).

[28] E. L. Shirley, Phys. Rev. B 54, 16464 (1996).

[29] D. Prendergast, S. G. Louie, *Bloch-state-based interpolation: An efficient generalization of the Shirley approach to interpolating electronic structure*, Phys. Rev. B 80, 235126 (2009).